https://doi.org/10.5194/amt-2019-215
Preprint. Discussion started: 16 July 2019

Atmospheric Measurement Techniques Discussions

Measurement of ammonia, amines and iodine species using protonated water cluster chemical ionization mass spectrometry

Joschka Pfeifer[1,2], Mario Simon[2], Martin Heinritzi[2], Felix Piel[2,a], Lena Weitz[2,b], Dongyu Wang[3], Manuel Granzin[2], Tatjana Müller[2], Steffen Bräkling[4], Jasper Kirkby[1,2], Joachim Curtius[2], and Andreas Kürten[2]

[1]CERN, Geneva, 1211, Switzerland
[2]Institute for Atmospheric and Environmental Sciences, Frankfurt Am Main, 60438, Germany
[3]Paul Scherrer Institute, Villigen, 5232, Switzerland
[4]TOFWERK AG, Thun, 3600, Switzerland

[a]now at: Ionicon Analytik GmbH, 6020 Innsbruck, Austria
[b]now at: GSI Helmholtzzentrum für Schwerionenforschung GmbH, Darmstadt, 64291, Germany

Correspondence to: Joschka Pfeifer (joschka.pfeifer@cern.ch)

Abstract. A new water cluster Chemical Ionization-Atmospheric Pressure interface-Time Of Flight mass spectrometer (CI-APi-TOF) is introduced. The instrument is designed for the selective measurement of trace gases with high proton affinity, such as ammonia, amines, and diamines that are, for example, relevant for atmospheric new particle formation. Following the instrument description and characterization, we demonstrate successful measurements at the CLOUD (Cosmics Leaving OUtdoor Droplets) chamber where very low ammonia background levels of ~4 pptv were achieved (at 278 K and 80% RH). The level of detection of the water cluster CI-APi-TOF can be estimated as ~0.5 pptv for ammonia and it is significantly lower for amines. Due to a short reaction time (< 1ms) and high primary ion concentrations in the cross-flow ion source even high ammonia mixing ratios of ca. 10 ppbv can be measured without significant reagent ion depletion. Besides the application to measure compounds like ammonia and amines, the technique is also suitable for the measurement of iodine oxides. During experimental runs exploring the nucleation capabilities of iodine-containing species in the CLOUD chamber, many different iodine-containing species were identified with the water cluster CI-APi-TOF. These compounds involved iodic acid and neutral clusters containing as many as four iodine atoms. However, the molecular structures of the measured iodine-containing species are not explicitly known, due to the difficulty in separating potential water molecules from the clusters. In addition to the description of the results obtained at the CLOUD chamber, we discuss the applicability of the technique for atmospheric measurements.

https://doi.org/10.5194/amt-2019-215
Preprint. Discussion started: 16 July 2019

Atmospheric Measurement Techniques Discussions

1 Introduction

Ammonia (NH_3) is an important atmospheric trace gas that is mainly emitted by agricultural activity due to animal husbandry and the use of fertilizers. It can partition to the aerosol phase and is one of the most important compounds contributing to secondary aerosol formation (Jimenez et al., 2009). Strong reductions in PM2.5 levels and the associated adverse health effects could potentially be achieved by decreasing agricultural emissions of ammonia (Pozzer et al., 2017). However, ammonia is not only partitioning to existing particles, but it can also be involved in the very first steps of new particle formation (nucleation) because it can stabilize newly-formed clusters in ternary (sulfuric acid-water-ammonia) and multi-component (sulfuric acid-water-ammonia-highly oxygenated organic molecules) systems (Kirkby et al., 2011; Kürten et al., 2016a; Lehtipalo et al., 2018). On a global scale, a large fraction of newly formed particles and cloud condensation nuclei involves ammonia (Dunne et al., 2016). The involvement of ammonia in nucleation has recently been measured in the free troposphere, in Antarctica, and in the boreal forest (Bianchi et al., 2016; Jokinen et al., 2018; Yan et al., 2018). In the upper troposphere, model calculations suggest that ammonia can also be important for new particle formation and their early growth (Dunne et al., 2016) and recent satellite measurements show that ammonia can be present at several tens of pptv (parts per trillion by volume) level over Asia (Höpfner et al., 2016). Ammonia has a very strong effect on nucleation involving sulfuric acid and water, e.g., recent studies have shown that very low amounts of NH_3 in the pptv-range, or even below, can enhance nucleation rates by orders of magnitude compared with the pure binary system of sulfuric acid and water (Kürten et al., 2016a; Kürten, 2019). Other basic compounds like amines or diamines, have been shown to enhance nucleation rates even stronger compared with ammonia despite their much lower atmospheric concentrations (Almeida et al., 2013; Kürten et al., 2014; Jen et al., 2016; Yao et al., 2016). The experimental measurements are in principle confirmed by quantum chemical calculations regarding the stabilizing effects of ammonia, amines, and diamines (Kurtén et al., 2008; Elm et al., 2017; Yu et al., 2018). For these reasons the measurement of ammonia, amines, and diamines is important in order to understand new particle formation and the partitioning between gas and aerosol phase. It is important to note that ammonia can easily exceed several ppbv in the boundary layer, whereas amine mixing ratios are typically present at a few pptv only (Hanson et al., 2011; You et al., 2014; Kürten et al., 2016b; Yao et al., 2016).

In some previous studies, ammonia has been measured using optical absorption or chromatographic methods (Norman et al., 2009; Bobrutzki et al., 2010; Verriele et al., 2012; Bianchi et al., 2012; Pollack et al., 2019). These measurement techniques are often specialized for the detection of only a few selected compounds, whereas chemical ionization mass spectrometry (CIMS) is a versatile tool for measuring atmospheric trace gases at low concentrations and high time resolution. The use of different reagent ions has been described in the literature for ammonia and amine measurements, e.g., protonated acetone, protonated ethanol, O_2^+, and protonated water clusters (Nowak et al., 2007; Norman et al., 2007; Benson et al., 2010; Hanson et al., 2011; You et al., 2014; Yao et al., 2016). Most of these techniques were used for ground-based measurements. Nowak et al. (2010) deployed their instrument on an aircraft for measurements at up to ~5 km altitude. The limit of detection (LOD)

https://doi.org/10.5194/amt-2019-215
Preprint. Discussion started: 16 July 2019


Atmospheric Measurement Techniques Discussions

varies between 35 pptv (You et al., 2014) and 270 pptv (Norman et al., 2009) for ammonia, whereas amines can be detected in the sub-pptv range (You et al., 2014; Sipilä et al., 2015; Simon et al., 2016).

In this study we introduce a newly developed chemical ionization mass spectrometer that uses protonated water clusters for selective ionization of ammonia, amines, and diamines. The mass spectrometer that is used is a high resolution Chemical Ionization-Atmospheric Pressure interface-Time Of Flight mass spectrometer (CI-APi-TOF, Aerodyne Inc. and TOFWERK AG) with a home-built ion source. The instrument is called water cluster CI-APi-TOF, naming it in accordance with other established techniques using the same mass spectrometer but different reagent ions, e.g., the nitrate CI-APi-TOF for sulfuric acid, highly-oxygenated organic molecule, and cluster measurements (Jokinen et al., 2012; Ehn et al., 2014; Kürten et al., 2014). The instrument is described and characterized; furthermore, its application during the CLOUD (Cosmics Leaving OUtdoor Droplets) chamber experiment at CERN (European Organization for Nuclear Research) is demonstrated. It is shown that the LOD reaches below 1pptv for ammonia, which is unprecedented to our knowledge.

Besides the measurement of basic compounds with high proton affinity we have discovered that the protonated water clusters are also well-suited to measure some iodine-containing species, e.g., HIO_3 and even clusters containing up to four iodine atoms. The corresponding signals in the mass spectra were identified during CLOUD experimental runs focusing on new particle formation processes induced by iodine-containing species. The relevance of such compounds for nucleation has recently been reported (Sipilä et al., 2016). A full list of the identified iodine species with their sum formulas is provided. However, their exact molecular structures is currently not clear. Our findings indicate that the water cluster CI-APi-TOF can yield important information on trace gases relevant for nucleation in different chemical systems involving, e.g., ammonia, amines and iodine species.

2. Methods

2.1 CLOUD chamber

Measurements shown in the present study were conducted at the CLOUD (Cosmics Leaving OUtdoor Droplets) chamber at CERN (European Organization for Nuclear Research) during fall 2017 (CLOUD12 campaign) and fall 2018 (CLOUD13 campaign). The CLOUD chamber is used to investigate new particle formation from different trace gas mixtures under atmospheric conditions regarding temperature, relative humidity, UV light intensity and ionization level (Kirkby et al., 2011; Kupc et al., 2011, Duplissy et al., 2016). The cylindrical stainless steel chamber has an inner volume of 26.1 m^3. It is designed to ensure that trace gas contaminant levels are low enough to allow precisely controlled nucleation experiments (Kirkby et al., 2016). The chamber is continuously flushed with synthetic air generated from liquid nitrogen and oxygen. Both, the temperature and the relative humidity of the gas inside the chamber can be precisely controlled. For the present study ammonia and dimethylamine from gas bottles were injected by a two-step dilution system (Simon et al., 2016; Kürten et al., 2016a). The calibration of the water cluster CI-APi-TOF with ammonia was carried out while the instrument was disconnected from the

https://doi.org/10.5194/amt-2019-215
Preprint. Discussion started: 16 July 2019

Atmospheric Measurement Techniques Discussions

chamber. For the calibration measurements the two-step dilution system from the CLOUD chamber was replicated (Figure 1 and Section 2.2).

Iodine is introduced into the chamber by nitrogen flowing over solid, molecular iodine (I_2, Sigma-Aldrich, 99.999% purity) placed in an evaporator bath that is heated up to 303 K. The generation of iodine-containing species for new particle formation is initiated from the photolysis of I_2 in the presence of ozone and water. Measurements presented in this work are carried out at temperatures between 223 and 298 K with relative humidity ranging between 10 and 90%. For the temperature measurements inside the CLOUD chamber, a Pt100 temperature sensor was used.

A chilled dew point mirror, manufactured by Edgetech Instruments, is used to measure the dew point inside the CLOUD chamber, where the relative humidity is derived by using water vapour pressure formulations published by Murphy and Koop (2005). Next to this, the relative humidity is measured by a Tunable Diode Laser system (TDL) developed by Karlsruhe Institute for Technology (KIT) that is installed at the mid plane of the chamber (Skrotzki, 2012). The relative humidity was derived using the mean value of both instruments, where a measurement uncertainty of 5% was assumed.

2.2 Water cluster CI-APi-TOF

The selective detection of ammonia and amines by atmospheric pressure chemical ionization using positively-charged water clusters has recently been demonstrated (Hanson et al., 2011). The same ionization technique is used in the present study. The reagent and product ions are measured with an Atmospheric Pressure interface-Time Of Flight mass spectrometer (APi-TOF), which is coupled with a newly-designed crossflow chemical ionization (CI) source operated at ambient pressure (Figure 1). The reagent ions, i.e., protonated water clusters ($(H_2O)_nH_3O^+$) are generated by positive corona discharge in the presence of argon (95 %), oxygen (5 %), and water vapor. The water vapor is added by bubbling the argon through a stainless steel humidifier (containing ca. 1 liter of purified water) held at ambient temperature of ~20 °C. As suggested by Hanson et al. (2011), a few droplets of sulfuric acid were added to the water in order to minimize potential contamination with ammonia from the water supply. Flow rates of 2.5 standard liters per minute (slm) for argon and 0.1 slm for oxygen were used, respectively. All flow rates were controlled by calibrated mass flow controllers (MFC). A conversion factor for the measured argon flow (provided by the MFC manufacturer) was applied. First attempts have been made using nitrogen instead of argon for the flow that passes the corona needle, but this resulted in much higher ammonia backgrounds. These backgrounds are most likely explained by NH_3 production in the corona plasma. Furthermore, the addition of oxygen is necessary for the generation of a stable corona discharge in positive mode when using argon as the main ion source gas (Weissler, 1943).

Protonated water is also used in proton-transfer-reaction mass spectrometry (PTR-MS) that has been described in numerous publications (Good et al., 1970; Kebarle, 1972; Zhao and Zhang, 2004; Hansel et al., 2018). A simplified reaction scheme leading to the formation of protonated water clusters is shown below (Sunner et al., 1988):

$$e^- + O_2 \rightarrow O_2^+ + 2\,e^-, \qquad \text{(R1)}$$

https://doi.org/10.5194/amt-2019-215
Preprint. Discussion started: 16 July 2019

Atmospheric Measurement Techniques Discussions

$$O_2^+ + (H_2O)_2 \rightarrow O_2^+(H_2O)_2 \rightarrow H_3O^+(OH) + O_2, \quad \text{(R2)}$$

$$H_3O^+(OH) + (H_2O)_n \rightarrow H_3O^+(H_2O)_n + OH. \quad \text{(R3)}$$

The PTR-MS operates its ion-molecule reaction zone typically at low pressure (~ 10 hPa) and uses an electric field (~ 100 V mm^{-1}) to break up water clusters such that mainly H_3O^+ ions react. The use of charged water clusters ($(H_2O)_{n\geq1}H_3O^+$ instead of H_3O^+) can increase the selectivity as water clusters have a much higher proton affinity compared with the water monomer (Aljawhary et al., 2013). However, due to their high proton affinity, ammonia and amines can still be detected according to the following reaction scheme:

$$H_3O^+(H_2O)_n + \mathrm{X} \rightarrow \mathrm{X}H^+(H_2O)_b + (n + 1 - b) \cdot (H_2O), \quad \text{(R4)}$$

where X represents the target substance that is ionized in the ion-molecule reaction zone (see below) and detected in the mass spectrometer. As water molecules can evaporate in the atmospheric pressure interface of the mass spectrometer, some of the product ions can be detected without water, e.g., ammonia is mainly detected as NH_4^+ (see Figure 2).

A schematic drawing of the ion source and the calibration setup is shown in Figure 1. The gas mixture for the ion source is composed of argon, oxygen and water vapor. It is introduced from two lines placed in the opposite direction to each other at an overall flow rate of ~2.6 slm. A voltage of 3600 V is applied to the corona needle while 500 V are applied to the conically-shaped counter electrode made of stainless steel. The housing of the ion source is made of polyether ether ketone (PEEK). The ion source gas and the generated reagent ions flow through a funnel (smallest inner diameter 2.5 mm) before they mix with the sample flow. A small capillary (inner diameter of 0.8 mm) is located opposite of the funnel. The electric field between the counter electrode and the capillary (at ground potential) accelerates the ions towards the entrance of the mass spectrometer. The pinhole plate (pinhole inner diameter of 350 µm) and the capillary are in electric contact and ~0.8 slm flow through the capillary and the pinhole into the mass spectrometer. The ion molecule reaction zone is defined by the distance between the counter electrode and the capillary (~ 16.4 mm). The estimated reaction time is <1 ms. This short reaction time allows the measurement of even high concentrations of ammonia (up to ~10 ppbv) without significant depletion of the reagent ions, which would be the case when using an ion source design as it has frequently been used during recent years for the measurement of sulfuric acid (Eisele and Tanner, 1993; Kürten et al., 2011), which is typically present at much lower concentrations than ammonia. The principle of a cross-flow ion source was introduced by Eisele and Hanson (2000) who used this technique to detect molecular sulfuric acid clusters. In more recent studies, this technique was used for the measurement of ammonia (Nowak et al., 2002; Nowak et al., 2006; Hanson et al., 2011). The inlet of the water cluster CI-APi-TOF consists of a stainless steel tube with 1 inch outer diameter that is housed by a stainless steel body that also holds the ion source and the counter electrode; additional parts made of PEEK insulate the electrodes. A total sample flow rate of ~ 19.5 slm is maintained by a

https://doi.org/10.5194/amt-2019-215
Preprint. Discussion started: 16 July 2019


Atmospheric Measurement Techniques Discussions

vacuum pump and a mass flow controller. The overall length of the sampling line connecting the CLOUD chamber and the ion molecule reaction zone is 1.3 m.

The measured volume mixing ratio (VMR, in pptv) of detected compounds is derived from a calibration factor (*C*) and the sum of the product ion counts per second (pcs) normalized against the sum of the reagent ion counts per second (rcs) (Kürten et al., 2016b; Simon et al., 2016):

$$VMR = C \cdot \ln\left(1 + \frac{\sum pcs}{\sum rcs}\right) = C \cdot ncps. \quad (1)$$

Equation (1) yields the VMR measured by the water cluster CI-APi-TOF as a function of the normalized counts per second (*ncps*). A calibration factor, *C*, that includes factors like the reaction rate and the effective reaction time, is required to convert the *ncps* to a mixing ratio. This factor can be derived from the inverse slope of a calibration curve (see Section 3.2). The only compound for which a direct calibration is performed in the present study is ammonia (Section 2.3). When mixing ratios for other basic compounds are presented the same calibration factor is used. This can in principle introduce uncertainty but at least for ammonia and amines the reaction rates for this type of ionization do not seem to be significantly different (Hanson et al., 2011). While Hanson et al. (2011) report a maximum for the water cluster distribution at the pentamer, evaporation of water seems to be stronger in our instrument. The maximum signal in clean spectra is usually found for the water dimer ($(H_2O)H_3O^+$, see Figure 2) and a strong drop in the reagent ion signals is found beyond the tetramer ($(H_2O)_3H_3O^+$). Therefore, the sample quantification includes, using ammonia as an example, the product ions $(H_2O)_nNH_4^+$ with n = 0,1 and the reagent ions $(H_2O)_mH_3O^+$ with m = 0-3. Possible losses of the analytes in the sampling line are not taken into account by the calibration factor (see Section 3.8 for discussion of sampling line losses).

2.3 Calibrations

2.3.1 Ammonia

Figure 1 shows a schematic drawing of the experimental setup during the calibrations with ammonia. The ammonia was taken from a gas bottle containing an NH_3 mixing ratio, *B*, of 100 ppmv (diluted in pure nitrogen) that is diluted in two steps, where MFCs are used to obtain different set points for the volume mixing ratio (Figure 1). During the second dilution step the mixture from the first dilution is injected into the center of the main sample flow (flow rate, Q_{sample}). The theoretical VMR_{theor} is given by (Simon et al., 2016):

$$\mathrm{VMR_{theor}} = \frac{\mathrm{MFC_1}}{\mathrm{MFC_1}+\mathrm{MFC_2}} \cdot \frac{\mathrm{MFC_3}}{\mathrm{MFC_3}+Q_{sample}} \cdot B. \quad (2)$$

MFC_1 (0.01 slm max.) describes the flow of ammonia from the gas bottle, whereas MFC_2 (2 slm range) controls the flow of nitrogen for the first dilution step. The flow of diluted ammonia that is introduced into the sample flow is controlled by MFC_3 (0.1 slm range). The calibration flow consists of the same synthetic air that is used for the CLOUD chamber.The flow is

https://doi.org/10.5194/amt-2019-215
Preprint. Discussion started: 16 July 2019


Atmospheric Measurement Techniques Discussions

provided by two MFCs that control a dry portion of the flow (MFC_{dry}, see Figure 1) and a wet portion of the flow that has passed a stainless steel water bubbler (MFC_{wet}, see Figure 1). By adjusting MFC_{dry} and MFC_{wet} (both 50 slm range) the RH of the sample flow can be controlled in order to test whether a humidity dependence exists for reaction (R4). Care is taken that the sum of MFC_{dry} and MFC_{wet} is always somewhat larger than Q_{sample}. To avoid pressure changes in the sampling line, the excess flow is vented through an exhaust before the sampling line.

Accordingly, the measured sample air consists of synthetic air (80% nitrogen, 20% oxygen) of varying humidity and the amount of ammonia injected to the system. To obtain calibration curves, the highest targeted calibration value is adjusted such that the maximum MFC_3 flow is used. The calibration points are then recorded by stepping down the MFC_3 flow. In this way, equilibration times are fairly short as the NH_3 mixing ratio before and directly after MFC_3 remains constant (see also Section 3.2).

2.3.2 Iodine Oxides

Besides the detection of ammonia and amines by the described ionization scheme, product ions from iodine-containing species were detected during new particle formation experiments initiated from I_2 photolysis during the CLOUD13 run. Prominent signals ($HIO_3 \cdot H^+$ and $HIO_3 \cdot H_3O^+$) corresponding to the neutral species of HIO_3 were observed among others (discussed in Section 3.5 and Table 2). These species can be unambiguously identified due to the large negative mass defect of the iodine atom and the high resolution (> 3000 Th/Th) of the mass spectrometer. No direct calibration for HIO_3 was performed; however, another chemical ionization mass spectrometer using nitrate reagent ions (nitrate CI-APi-TOF) was also measuring HIO_3 at CLOUD. Therefore, a calibration factor for HIO_3 is derived by scaling concentrations measured by the nitrate CI-APi-TOF that is calibrated for sulfuric acid (Kürten et al., 2012). We further assume that both sulfuric and iodic acid are detected with the same efficiency by the nitrate CI-APi-TOF. For the instrument inter-comparison (and the indirect calibration of the water cluster CI-APi-TOF), 18 different CLOUD experimental runs were chosen and mean values were calculated for different steady-state concentrations. We took 6 steady-state concentrations each at temperatures of 263 K (80% relative humidity) and 283 K (40% relative humidity and 80% relative humidity).

2.4 PICARRO

A PICARRO G1103-t NH_3 Analyzer (PICARRO Inc., USA) measured ammonia and water vapor mixing ratios based on cavity-ring down spectroscopy during CLOUD12 and CLOUD13. The instrument is suitable for real-time monitoring of ammonia in ambient air and has been presented in previous studies (Bell et al., 2009). The G1103-t was installed at the CLOUD chamber with its own sampling line coated with Sulfinert (Restek GmbH, Germany), where the coating reduced the losses of ammonia to the sampling line walls considerably. For some inter-comparison measurements the PICARRO was connected to the exhaust line of the water cluster CI-APi-TOF. Since the PICARRO has a rather small sample flow rate (~0.3 slm), an additional pump was used to enhance the flow rate to 5 slm just before the instruments inlet. This was done in order to minimize line losses and to decrease the response time. It was, however, not quantitatively tested in how far these measures (Sulfinert

https://doi.org/10.5194/amt-2019-215
Preprint. Discussion started: 16 July 2019

Atmospheric Measurement Techniques Discussions

and increased flow rate) helped with the measurements. The PICARRO was also independently calibrated with a NH_3 permeation tube (Fine Metrology, Italy) using a multigas calibrator (SONIMIX 6000 C1, LNI Swissgas, Switzerland). The time interval for one measurement of the PICARRO is 5 seconds for which a lower detection limit of 200 pptv is reported (PICARRO Inc., USA; Martin et al., 2016).

3. Results and Discussion

3.1 Main peaks in spectrum

Figure 2 shows a typical spectrum during calibrations, where 10 ppbv of ammonia are injected (40% relative humidity, ~293 K). The dominating detected primary ions are H_3O^+, $(H_2O)H_3O^+$ and $(H_2O)_2H_3O^+$. $(H_2O)H_3O^+$ is the dominant primary ion in the mass spectrum. The water tetramer ($(H_2O)_3H_3O^+$) is usually the largest water cluster that can be detected. The addition of ammonia generates NH_4^+ and $(H_2O)NH_4^+$; a small signal from NH_3^+ is also visible. At low ammonia concentrations the signal from NH_4^+ can have a similar magnitude compared with the signal from H_2O^+ (possibly from reactions of O_2^+ and H_2O). Since these ions have the same integer mass, a high mass resolving power is essential in terms of reaching low detection limits as otherwise the differentiation between the two signals is not possible. At the low masses the APi-TOF used in the present study reaches a resolving power of ~2000 Th/Th, which is sufficient to separate the two peaks. For the analysis of the spectra, the software TOFWARE is used that allows us to analyze high resolution spectra (Harald Stark et al., 2015; Cubison and Jimenez, 2015; Timonen et al., 2016). Prominent peaks from N_2H^+, NO^+ and O_2^+ can also be found in the spectrum shown in Figure 2. It is not clear how these ions are formed and why they survive the relatively long reaction time of ~1 ms since Good et al. (1970) report that O_2^+ reacts rapidly away in moist air. For the analysis the presence of these background peaks is currently ignored and they are not counted as reagent ions (in equation (1)) as no evidence exists that they interact with the target species relevant for the present study. An exception could be NH_3^+ (possibly from reaction of O_2^+ and NH_3); but NH_3^+ is not considered and is only a small fraction of NH_4^+.

In contrast to the spectrum shown in Figure 2 with relatively small water clusters, Hanson et al. (2011) observe the highest signal in the water cluster distribution for the pentamer. We explain this difference in more pronounced fragmentation and evaporation of ion clusters in the atmospheric pressure interface of our mass spectrometer.

For estimating an ammonia mixing ratio according to equation (1), the product ion count rates are normalized against the dominating reagent ion count rates. Figure 2 shows that even at 10 ppbv of injected ammonia the reagent ion signals are significantly higher than the product ion count rates. This indicates that no significant reagent ion depletion occurs and thus the calibration factor (C) describes the measured ammonia VMR linear when applied to the normalized counts per second with sufficient precision at least up to 10 ppbv (see Section 3.2).

https://doi.org/10.5194/amt-2019-215
Preprint. Discussion started: 16 July 2019

Atmospheric Measurement Techniques Discussions

3.2 Ammonia and iodic acid calibration

Figure 3 shows the calibration curves obtained for NH_3 and HIO_3 (for the CLOUD13 campaign). Each dot represents the mean value of a steady state measurement of at least 20 minutes. The normalized counts per second are based on the two highest signals assigned to the analyzed compound (ammonia: NH_4^+ and $(H_2O)NH_4^+$; iodic acid: HIO_3H^+ and $HIO_3H_3O^+$). The total error of the VMR (on the *x*-axis) is calculated by Gaussian error propagation taking into account the standard deviation of the flow rates from the mass flow controllers and the error of the VMR inside the ammonia gas bottle, where an error of ±5% is stated by the vendor. Since we obtained the VMR shown in Figure 3b by scaling the concentrations measured by a nitrate CI-APi-TOF calibrated for sulfuric acid, the error on the *x*-axis equals the uncertainty of these measurements (estimated as a factor of two for the iodic acid concentration). The error on the *y*-axis is given by the standard deviation of the normalized counts per second.

We derive a calibration curve that is most accurately described by a linear regression model using the Wilkinson-Rogers Notation (Wilkinson and Rogers, 1973). The fit was forced through the origin; however, even when the fit is not constrained, the resulting slope is essentially the same (the results differ by only several ppm). The derived slopes represent the inverse of the calibration factor, C (~ 1.46×10^5 pptv at 40% RH), in equation (2). Figure 3 shows that all measured concentration steps lie in the area of the confidence bounds (95% confidence intervals) and thus the linear model describes the dependency very well. The calibration was performed before the CLOUD13 experiment (Sept. 2018), during and after the experiment (Dec. 2018) at different levels of humidity (calculated relative humidity levels between ~3% and 82%) and ambient temperatures.

The calibrations for ammonia were performed by introducing the highest mixing ratio first. However, even at the highest mixing ratio, it took almost a day to reach stable signals as the tubing and the two MFCs through which the ammonia was flown (MFC_1 and MFC_3) needed to equilibrate. The further calibration points were then recorded by reducing the flow rate of MFC_3. In this way, no change in the ammonia mixing ratio inside the capillary before the main sampling line was necessary. This allowed for a relatively fast stepping through the calibration set points. However, even when the ammonia flow was shut-off there was still significant diffusion of ammonia from the capillary into the sampling line, which resulted in relatively high background values (with nominally zero NH_3). For this reason, we derived the limit of detection by measuring the background of the CLOUD chamber with the calibration lines removed (Section 3.4). During the calibrations, the relative humidity was calculated by assuming that the sample flow passing the water reservoir is saturated with water (Figure 1). For the calibrations carried out after the campaign, the temperature of the total sample flow was measured to derive the absolute humidity. The calibration points in Figure 3 were taken at measured gas flow temperatures of 288 to 290 K. The relative humidity was set to 40% RH by adjusting the dry and the wet flow rates for the sample flow; these conditions correspond to an absolute humidity of ~ 0.0057 kg m^{-3}.

The calibration factor derived for CLOUD12 (for ammonia) differs from the calibration factor shown here. This is due to the slightly different ion source, that is, e.g., adjusted to a 0.5 inch sampling line diameter instead of one inch. Next to the different dimensions, the voltages of the quadrupoles inside the mass spectrometer, as well as the flow rates and the voltages

https://doi.org/10.5194/amt-2019-215
Preprint. Discussion started: 16 July 2019


Atmospheric Measurement Techniques Discussions

285 applied to the ion source were different compared to the CLOUD13 campaign leading to small changes in sensitivity and resolution.

3.3 Influence of the humidity on the sensitivity

Figure 4 shows the sensitivity dependence for the ammonia measurements with varying relative humidity. These data points
290 are derived from calibration curves similar to the one shown in Figure 3a. However, during the calibrations the humidity was changed by adjusting the dry and wet sample flow rates. For all conditions NH_4^+ has the highest product ion count rate. However, the ratio of the signals for $(H_2O)NH_4^+$ and NH_4^+ increases with humidity as well as the sensitivity. A possible explanation for the observed sensitivity dependence could be increased collision rates at high humidity where larger water clusters are present. In addition, the detection efficiency of the mass spectrometer (including all components) does not have a
295 constant detection efficiency over the full mass range (Heinritzi et al., 2016). A higher detection efficiency at *m*/*z* 36 ($(H_2O)NH_4^+$) compared with *m*/*z* 18 (NH_4^+) together with the higher fraction of $(H_2O)NH_4^+$ compared with NH_4^+ at high humidity could explain some of the observed effect. In the end, however, the observed increase in sensitivity is not dramatic (increase by a factor of ~2.5 when the humidity increases by a factor of 10). Nevertheless, the effect is taken into account by using the measured relative humidity inside the CLOUD chamber (see Section 2.42) to correct the derived ammonia mixing
300 ratio.

The effect of temperature on the sensitivity could not be tested during a dedicated calibration experiment as our calibration setup is not temperature-controlled. However, during one of the CLOUD runs a constant amount of ammonia (~10 ppbv) was injected while the chamber was cooled down from 298 to 248 K at constant relative humidity. Unfortunately, the instrument was only connected shortly before the experiment started; therefore, a drift of the signal of ca. 15% was observed in the
305 beginning. At a later stage the change in the signal was below 3% during the temperature transition from 278 K to 250K. This indicates that the temperature dependency is negligible when the relative humidity stays constant.

The dependency of the sensitivity with relative humidity and temperature is different for the measurement of iodic acid as shown in Figure 5. While NH_4^+ (without a water molecule) is the dominant signal for ammonia, $H_4IO_4^+$ ($H_2O{\cdot}HIO_3H^+$ or $HIO_3{\cdot}H_3O^+$) yields the highest signal for iodic acid (higher than HIO_3H^+). We observed an increasing sensitivity at lower
310 temperatures, while the humidity dependency appears to be smaller compared to the ammonia measurements (Figure 4). The higher count rate of $H_4IO_4^+$ compared to $H_2IO_3^+$ could indicate that iodic acid requires additional water in order to be associated with a positively charged ion. However, during the transition from ambient pressure into the vacuum of the mass spectrometer, water molecules can evaporate and leave $H_2IO_3^+$ in a non-equilibrium process. Besides the observation of iodic acid, additional signals from iodine-containing species can be found in the spectra. These species are listed in Table 2.
315 Elucidating the exact formation pathways of these ions and the corresponding neutral species is subject for future work.

https://doi.org/10.5194/amt-2019-215
Preprint. Discussion started: 16 July 2019


Atmospheric Measurement Techniques Discussions

3.4 Detection limits

Determining the limit of detection (LOD) for ammonia is not trivial as the background signal is not constant. During the calibrations a relatively high background was observed, which was usually decreasing slowly after the ammonia flow through the capillary was shut off. A typical value reached a couple of minutes after the ammonia flow was turned off is ~30-60 pptv. When the water cluster CI-APi-TOF was connected to the CLOUD chamber the NH_3 signals usually dropped significantly when no ammonia was actively added. However, even under these conditions the ammonia was not zero and the measured signal changed when the RH or temperature of the chamber was adjusted. There is evidence that the contaminant level of the CLOUD chamber with respect to ammonia is on the order of several pptv at 278 K and 38% RH (Kürten et al., 2016a). During CLOUD13 the measured background (at 278 K and 80% RH) was 3.7 pptv, which in principle confirms the previous estimates. The fact that the sampling line of the instrument can also be a source of contamination could explain the somewhat higher value. Another source of background ammonia could be the ion source. During the early stages of our development we used nitrogen instead of argon as the main ion source gas. This lead to ammonia backgrounds on the order of hundreds of pptv. The exact formation pathway of ammonia from N_2 (and other traces gases including oxygen and water vapor) is not clear to us. However, replacing nitrogen with argon quite drastically decreased the background ammonia signals. Still, traces of nitrogen containing gases in the ion source could contribute to the ammonia background. For the present study we report a background ammonia mixing ratio of 3.7 pptv (Table 1) for 278 K and 80% RH but note that the background is significantly lower for lower temperature, which argues against the ion source being a significant source of ammonia since it is always at ambient temperature. An increase in relative humidity increases the measured ammonia mixing ratio because water molecules can displace adsorbed ammonia on the chamber walls and the sampling line (Vaittinen et al., 2014).

The LOD is defined as the additional ammonia mixing ratio that is necessary to exceed three times the standard deviation at background conditions (You et al., 2014). This value corresponds to 0.5 pptv for an averaging time of 1 minute. Assuming the same sensitivity as for ammonia and taking into account the background signals for the exact masses, LODs for other compounds can be estimated. Besides the values for ammonia, Table 1 lists the derived backgrounds and LODs for C_2-amines (e.g., dimethylamine), pyridine and iodic acid. The evaluation of high resolution data is necessary for deriving the values shown in Table 1 as for some compounds several species occur at the same integer mass. E.g., for the C_2-amines (exact mass of protonated compounds at 46.0651 Th) other species like NO_2^+ (45.9924 Th) or CH_4NO^+ (46.0287 Th) can interfere. For pyridine and C_2-amines only the peak with the highest count rate is taken into account, since $(C_5H_5N)H_3O^+$ and $(C_2H_7N)H_3O^+$ interfere with other compounds measured during the experiments even when using high resolution data. In principle, the omission of the larger product ions (with one additional water molecule) should lead to a different calibration constant. However, the effect is small as the ion signals with the associated water are smaller than the products without the water molecule for the measured bases.

The instrumental background for NH_3 is higher than the backgrounds of the other compounds shown in Table 1. This might be the case, since low levels of NH_3 are more difficult to achieve due to the ubiquitous presence of ammonia. In any case, the

https://doi.org/10.5194/amt-2019-215
Preprint. Discussion started: 16 July 2019


Atmospheric Measurement Techniques Discussions

detection limit derived for ammonia is well below the LOD reported for other measurement techniques and instruments (Bobrutzki et al., 2010; You et al., 2014; Lin; Wang et al., 2015). However, the performance of the water cluster CI-APi-TOF during atmospheric measurements remains to be tested. The signal of pyridine and C_2-amines is most of the time below the estimated limit of detection. However, in case of elevated signals, these seem to correlate with the corresponding natural ions in the CLOUD chamber measured by an APi-TOF in positive mode.

The detection limit of iodic acid is well below the LOD calculated for ammonia and C_2-amines (Table 1). We might explain this when looking at signals that could possibly interfere with the measured compounds. All compounds shown in Table 1 have an integer mass, where other signals are also detected, e.g. H_2O^+ at the nominal mass of ammonia, or NO_2^+ at the nominal mass of C_2-amines. These interfering signals can lead to increased detection limits. Next to this, we expect the transmission to be ~2 times higher for ions of mass to charge ratios of ~140-180 compared to ions of mass to charge ratios of ~18 to 60 according to a preliminary transmission curve characterization (data not shown) using the technique by Heinritzi et al. (2016). Thus, the sensitivity for compounds of masses in this region should increase. Finally, iodic acid has a much lower vapor pressure compared with ammonia and is not emitted efficiently from surfaces at temperatures relevant for the present study. Therefore, much lower backgrounds can be expected even if the sampling line and the instrument were exposed to high concentrations before.

3.5 Identified iodine species during CLOUD13

The signals for HIO_3 measured by the water cluster CI-APi-TOF show an excellent correlation with the iodic acid concentration from the nitrate CI-APi-TOF measuring in negative ion mode (see Figure 3b). Additionally, we were able to detect iodine-containing species at higher mass to charge ratios (e.g., iodine pentoxides) during several experimental runs. Figure 6 shows the detected iodine-containing species during an experimental run, when a high iodine concentration was injected into the chamber (mean values over a duration of 120 minutes). The mean iodic acid mixing ratio is at ~0.98 pptv according to the measurements of the water cluster CI-APi-TOF. During this time period, we observed iodine-containing species up to the tetramer (the terms monomers, dimers, trimers, and tetramers indicate the number of iodine atoms in the observed signals). The size of the circles shown in Figure 6 corresponds to the mean count rate of the signals on a logarithmic scale. For comparison, the intensities of the reagent ions are also shown. To provide more details on the observed signals, Table 2 lists the sum formulas of some identified iodine species.

During some runs, an electric field was applied to the chamber to get rid of ions and cluster ions for the study of purely neutral (i.e., uncharged) nucleation. Even during these experiments the signals as displayed in Figure 6 were present. This indicates that the water cluster CI-APi-TOF measures neutral compounds after ionizing them in the ion-molecule reaction zone. This study only gives a short overview of the iodine signals observed so far with the water cluster CI-APi-TOF. Further CLOUD publications will focus on the chemistry of the iodine-containing species and on their role in new particle formation processes.

https://doi.org/10.5194/amt-2019-215
Preprint. Discussion started: 16 July 2019

Atmospheric Measurement Techniques Discussions

3.6 CLOUD chamber characterization

The performance of the water cluster CI-APi-TOF during measurements at CLOUD12 is shown in Figure 7. We compare the derived mixing ratios with the measurements of the PICARRO. In addition, both measurements are compared with an estimated range of ammonia mixing ratios based on the injected amount of NH_3 into the CLOUD chamber, the chamber volume and the ammonia lifetime (see, e.g., Simon et al. (2016) and Kürten et al. (2016a) for the equations linking these quantities to the estimated CLOUD mixing ratios). While the injected ammonia can easily be determined from the MFC settings, the ammonia lifetime in the chamber can span a wide range. For a very clean chamber or at very low temperatures the chamber walls can essentially represent a perfect sink ("wall loss lifetime") and the ammonia has a short lifetime. A wall loss lifetime of 100 s at 12% fan speed was previously reported by Kürten et al. (2016a). Measurements of sulfuric acid at different fan speeds suggest a change of a factor of 4 in mixing ratios when the fan speed is changed from 12% to 100%. Scaling these measurements to the ammonia measurements yields a wall loss lifetime of 25 s at 100% fan speed. On the other hand, once the walls have been exposed for a long time with ammonia they reach eventually an equilibrium where condensation and evaporation rates become balanced. Under these conditions, the ammonia lifetime is determined by the dilution lifetime alone (5000 s), and so the NH_3 increases to higher equilibrium concentrations. Next to this, the walls can act as a source of ammonia due to re-evaporation of ammonia molecules attached to the surface. This effect is more significant when the concentrations previously injected to the chamber were higher, than the current concentrations. Thus, the estimated range can vary by a factor of ~200 based on the chamber conditions. This wide range is indicated by the shaded areas in Figure 7 (light blue color).

Figure 7a shows the measurements of the water cluster CI-APi-TOF, the PICARRO, and the calculated value for ammonia. The signal measured by the water cluster CI-APi-TOF follows the injected ammonia almost instantaneously (first injection is on Oct. 23), whereas the PICARRO only shows elevated concentrations above its background of ~200 pptv much later. This is due to the much higher LOD of the PICARRO and its much higher sampling line losses that require a considerably longer time for equilibration. After the flow of ammonia is shut -off, both the mass spectrometer and the PICARRO show almost identical values when the chamber is being cleaned. Before the first ammonia injection it can also be seen that the water cluster CI-APi-TOF shows progressively lower background ammonia values. Whether this is due to the chamber, the instrument or the sampling line becoming cleaner is unclear. Figure 7a also indicates the influence of temperature on the background ammonia. When the chamber temperature drops from 298 K to 278 K (shortly before Oct. 31) the residual NH_3 decreases by around a factor of 5, which is caused by a reduction in the re-evaporating ammonia from the chamber walls. Due to the higher LOD, the PICARRO, however, can hardly detect this decrease in the VMR.

Figure 7b shows how the ammonia mixing ratios inside the CLOUD chamber react on changes of the fan speed. The fan speed was varied between 12% (default value) and 100% to realize different wall loss rates of condensable species. As the temperature in this example is low (248 K) and the chamber is rather clean the walls act as a perfect sink for ammonia. Therefore, the measured mixing ratios almost instantaneously react to the changing fan speed indicating a change of a factor

https://doi.org/10.5194/amt-2019-215
Preprint. Discussion started: 16 July 2019


Atmospheric Measurement Techniques Discussions

4 in the mixing ratios. Thus, the measurements coincide with the calculated lifetimes. The PICARRO is insensitive at these low mixing ratios and cannot respond to conditions that change quickly.

3.7 Ammonia wall loss rates in the sampling line

The largest uncertainty in the ammonia measurement is related to the sampling line losses. At CLOUD, the sampling line is kept as short as possible, but the total length is still 1.3 m because the sampling line protrudes into the chamber over a distance of 0.5 m in order to sample air from the well-mixed center region of the chamber. Additionally, the sampling line has to traverse the structures for temperature control and heat insulation around the inner chamber walls. Using an ammonia diffusivity of 0.1978 $cm^2\ s^{-1}$ (Massman, 1998) and a sample flow rate of 20 slm, the sample line penetration efficiency can be estimated as 33.7% for a laminar flow (Dunlop and Bignell, 1997; Baron and Willeke, 2001; Yokelson, 2003). This means, that if the walls of the sampling line act as a perfect sink, then the measured NH_3 mixing ratios would need to be corrected with a factor of ~3. However, it is quite likely that the sampling line not always acts as a perfect sink for ammonia. Vaittinen et al. (2014) studied the adsorption of ammonia on different surfaces and found a value of 1.38×10^{14} molecule cm^{-2} for the surface coverage on stainless steel. For humid conditions this value is, however, significantly smaller and drops to $\sim5\times10^{12}$ cm^{-2} for a water vapor mixing ratio of 3500 ppmv at 278 K which can be explained by the displacement of ammonia by water molecules (Vaittinen et al., 2014).This indicates that, depending on the ammonia mixing ratio and the gas conditions (temperature and RH), eventually an equilibrium can be reached between the gas and the surface. In such a case, no wall loss correction would be necessary. Furthermore, ammonia may re-evaporate from the inlet line walls if saturation happened at higher concentrations previously. Unfortunately, it is therefore not straightforward to predict what the influence of the sampling line is as a function of time and pre-conditioning of the inlet line. One practical solution would be to report average values without correction and with the correction factor applied. These averages yield a range of possible values for the wall loss rates in the sampling line. When going from high values to low values, the sampling line walls can also become a source of ammonia. This can potentially lead to a strong over-estimation of the measured value and it can take a long time until the sampling line becomes clean enough to reach a new equilibrium.

We are aware that the sampling line losses introduce some uncertainty on the ammonia measurement. However, this is an effect other in-situ techniques also have to struggle with (see, e.g., Leifer et al. (2017)). We also want to note that the effect is much smaller for larger molecules, e.g., the penetration for triethylamine (diffusivity of 0.067 $cm^2\ s^{-1}$, Tang et al. (2015)) reaches 61%. For atmospheric measurements, we suggest to use an inlet system where a short piece of the 1'' sampling line only takes the core sample flow from a large diameter inlet. A blower can generate a fast flow in the large inlet to essentially reduce the losses for the core flow to zero before it enters the actual sampling line (Berresheim et al., 2000).

3.8 Measurements of amines

Figure 8a shows a measurement of the chamber background for C_2-amines (dimethylamine) carried out during CLOUD13 over a time period of 5 days. As mentioned in Section 3.4, the same calibration factor derived for ammonia was used to estimate

https://doi.org/10.5194/amt-2019-215
Preprint. Discussion started: 16 July 2019


Atmospheric Measurement Techniques Discussions

the mixing ratio of C_2-amines. The mean instrumental background for the time period shown in Figure 8a is ~0.14 pptv (for a temperature of 278 to 290 K and a relative humidity between ~50 and 60 %). The background values shown here are close to the background values obtained for 80% RH and 278 K (see Table 1). The observed variations are in a range of ~100 to 300 ppqv provided that the measurement is not interrupted, e.g., due to the replenishment of the water source that humidifies the flow for generating the reagent ions (which is shown in the first drop of the background measurement in figure 8a). The values shown here are below or at similar instrumental backgrounds reported in previous publications (You et al., 2014; Simon et al., 2016).

The measured values with the water cluster CI-APi-TOF are compared to calculated mixing ratios for a period when dimethylamine was actively injected into the CLOUD chamber. A chamber characterization for dimethylamine was already conducted by Simon et al. (2016), where the lifetime ranged from 432 s (perfect sink where, in the present work, a wall loss lifetime of 108s was used at fan speeds of 100 %, see section 3.6) to 8600 s (chamber dilution lifetime for CLOUD13 is 5000s). We used these values and the flows from the CLOUD dimethylamine gas dilution system (similar to Section 3.6 for ammonia) to estimate the expected mixing ratios for some experiments during the CLOUD13 campaign. Figure 8b shows the time period when dimethylamine was added. Since it takes a certain time until the stainless steel pipes of the gas dilution system are saturated with dimethylamine there is a short time delay between the switching of a valve that allows dimethylamine to enter the chamber and the rise in the measured dimethylamine mixing ratio. Once the lines are conditioned and the dimethylamine is homogenously mixed into the chamber, the measured and calculated mixing ratios are generally in good agreement with each other. This is especially the case when considering that no wall loss correction for the water cluster CI-APi-TOF is taken into account. Such a correction (estimated as a factor ~2) would raise the measured values and bring the values into even better agreement. This analysis indicates that the calibration factor for dimethylamine should not differ significantly from the value for ammonia. Fluctuations in the measured mixing ratio can be explained by changes in the fan speed. The deviations at the end of the time series shown in Figure 8b are caused by nucleation experiments in which high concentrations of other vapors are used. During these stages a significant uptake of dimethylamine on particles can explain the discrepancy between measured and expected dimethylamine.

4. Discussion and application to ambient measurements

The present study demonstrates the successful application of a water cluster CI-APi-TOF during controlled chamber experiments for ammonia, amine and iodine oxide measurements. The technique has unprecedented low detection limits regarding the ammonia measurement as well as a fast time response and time resolution. A next step is its application to atmospheric measurements. The technique should be suitable for such measurements as the amount of clean gas required (ca. 2 slm of argon and some oxygen) is rather small and can easily be supplied with gas bottles (one argon gas bottle, 50 liters at 200 bar should last ~3 days). At CLOUD there is a restriction regarding the maximum sample flow that can be taken from the

https://doi.org/10.5194/amt-2019-215
Preprint. Discussion started: 16 July 2019


Atmospheric Measurement Techniques Discussions

chamber. During atmospheric measurements much higher flow rates can easily be realized. Therefore, the suggested design of the inlet system using a blower and a core sample inlet should be used (see Section 3.8). Furthermore, the use of an internal calibration standard would be beneficial. We have tried to add a defined mixing ratio of ND_3 to the sample flow. However, besides the expected signal at (ND_3H^+, *m*/*z* 21) further signals corresponding to NH_4^+, NDH_3+, $ND_2H_2^+$ were also visible in the spectra due to deuterium-hydrogen exchange, which makes this method unfavorable. Use of $^{15}NH_3$ for calibration is also unfavorable since the $^{15}NH_4^+$ signal is hard to distinguish from the comparatively high H_3O^+ signal at the same integer mass even with a high resolution mass spectrometer.

Roscioli et al. (2016) demonstrated that the addition of 1H,1H-perfluorooctylamine to the sample flow can be used to passivate an inlet, which leads to greatly reduced sampling line losses and improved time response during ammonia measurements. Recently, Pollack et al. (2019) implemented this passivation technique for ambient measurements on an aircraft. For these measurements, a tunable infrared laser was used (TILDAS-CS, Aerodyne Inc.). We also tested the passivation technique, however, the high mixing ratio of 1H,1H-perfluorooctylamine (~100 ppm to 0.1% injection into the sample flow) that is required led to a consumption of the reagent ions since 1H,1H-perfluorooctylamine has a high proton affinity and is therefore also efficiently ionized by the protonated water clusters. For this reason, the passivation technique for the measurement of ammonia can in our opinion only be used with spectroscopic techniques as it was the case in the studies by Rosciolli et al. (2016) and Pollack et al. (2019).

5. Summary and Conclusion

The set-up and characterization of a water cluster Chemical Ionization-Atmospheric Pressure interface-Time Of Flight mass spectrometer (CI-APi-TOF) is described. The instrument includes a new home-built cross-flow ion source operated at atmospheric pressure. The generated protonated water clusters ($(H_2O)_{n\geq1}H_3O^+$) are used to selectively ionize compounds of high proton affinity at short reaction times. The instrument's response is linear up to a mixing ratio of at least 10 ppbv for ammonia when the derived calibration factor is applied to the normalized counts per second. The water cluster CI-APi-TOF was used at the CLOUD chamber where very low background ammonia mixing ratios (ca. 4 pptv) were achieved. The level of detection (LOD) was estimated as 0.5 pptv for NH_3. To our knowledge, such a low detection limit for ammonia measurements has not been reported so far. We attribute the low LOD mainly to the use of ultraclean argon (5.0 purity) as the main ion source gas for the reagent ion generation. Much higher background NH_3 was observed when using nitrogen instead of argon. Although, the sensitivity towards the measurement of NH_3 depends somewhat on the relative humidity of the sample flow, the observed sensitivity changes were rather low and can be taken into account by a correction factor. We did not explicitly demonstrate the quantitative measurement of diamines (and other amines than C_2 amines) in the present study but the instrument should also be well-suited for such measurements.

https://doi.org/10.5194/amt-2019-215
Preprint. Discussion started: 16 July 2019

Atmospheric Measurement Techniques Discussions

During some of the experiments involving iodine, it was observed that the protonated water clusters can also be used to detect various iodine species. A total of 29 different iodine-containing compounds were unambiguously identified, including iodic acid (HIO_3) and neutral clusters containing up to four iodine atoms. The water cluster CI-APi-TOF was cross-calibrated against a nitrate CI-APi-TOF measuring iodic acid during CLOUD. The two instruments showed exactly the same time-dependent trends and the LOD for the water cluster CI-APi-TOF was as low as 7 ppqv. Further CLOUD publications will focus on the iodine system.

Next to this, future studies will focus on the evaluation of the iodine signals and also on further signal identification in the mass spectra. Due to the instrument characteristics, we plan to apply the method to ambient atmospheric measurements to study the influence of ammonia, amines, diamines, and iodic acid on new particle formation. Airborne measurements in the upper troposphere, where very low ammonia mixing ratios can be expected (Höpfner et al., 2016) should in principle be feasible as well. Such measurement would be promising due to the extremely low LOD of the instrument.

Acknowledgements

We would like to thank CERN for the support of CLOUD with financial and technical resources. We thank the PS/SPS team from CERN for providing the CLOUD experiment with a particle beam from the proton synchroton. We also want to thank L.-P. De Menezes for providing us with a mass flow controller used during the calibrations. Next to this, we would like to thank R. Sitals, T. Keber, S. Mathot, H.E. Manninen, A. Onnela, S. K. Weber and R. Kristic for their contributions to the experiment. The discussion with Xucheng He during the creation of the paper is gratefully acknowledged. This work was funded by: the German Federal Ministry of Education and Research "CLOUD-16" (no. 01LK1601A), EC Horizon 2020 MSCA-ITN "CLOUD-MOTION" (no. 764991), and EC Seventh Framework Programme MC-ITN "CLOUD-TRAIN" (no. 316662).

https://doi.org/10.5194/amt-2019-215
Preprint. Discussion started: 16 July 2019

Atmospheric Measurement Techniques Discussions

References

Aljawhary, D., Lee, A. K. Y., and Abbatt, J. P. D.: High-resolution chemical ionization mass spectrometry (ToF-CIMS): application to study SOA composition and processing, Atmos. Meas. Tech., 6, 3211–3224, doi:10.5194/amt-6-3211-2013, 2013.

Almeida, J., Schobesberger, S., Kürten, A., Ortega, I. K., Kupiainen-Määttä, O., Praplan, A. P., Adamov, A., Amorim, A., Bianchi, F., Breitenlechner, M., David, A., Dommen, J., Donahue, N. M., Downard, A., Dunne, E., Duplissy, J., Ehrhart, S., Flagan, R. C., Franchin, A., Guida, R., Hakala, J., Hansel, A., Heinritzi, M., Henschel, H., Jokinen, T., Junninen, H., Kajos, M., Kangasluoma, J., Keskinen, H., Kupc, A., Kurtén, T., Kvashin, A. N., Laaksonen, A., Lehtipalo, K., Leiminger, M., Leppä, J., Loukonen, V., Makhmutov, V., Mathot, S., McGrath, M. J., Nieminen, T., Olenius, T., Onnela, A., Petäjä, T., Riccobono, F., Riipinen, I., Rissanen, M., Rondo, L., Ruuskanen, T., Santos, F. D., Sarnela, N., Schallhart, S., Schnitzhofer, R., Seinfeld, J. H., Simon, M., Sipilä, M., Stozhkov, Y., Stratmann, F., Tomé, A., Tröstl, J., Tsagkogeorgas, G., Vaattovaara, P., Viisanen, Y., Virtanen, A., Vrtala, A., Wagner, P. E., Weingartner, E., Wex, H., Williamson, C., Wimmer, D., Ye, P., Yli-Juuti, T., Carslaw, K. S., Kulmala, M., Curtius, J., Baltensperger, U., Worsnop, D. R., Vehkamäki, H., and Kirkby, J.: Molecular understanding of sulphuric acid-amine particle nucleation in the atmosphere, Nature, 502, 359–363, doi:10.1038/nature12663, 2013.

Baron, P. A. and Willeke, K.: Aerosol measurement: Principles, techniques, and applications, 2nd ed., Wiley, New York, xxiii, 1131, 2001.

Bell, C. L., Dhib, M., Hancock, G., Ritchie, G. A. D., van Helden, J. H., and van Leeuwen, N. J.: Cavity enhanced absorption spectroscopy measurements of pressure-induced broadening and shift coefficients in the υ 1+υ 3 combination band of ammonia, Appl. Phys. B, 94, 327–336, doi:10.1007/s00340-008-3238-5, 2009.

Benson, D. R., Markovich, A., Al-Refai, M., and Lee, S.-H.: A Chemical Ionization Mass Spectrometer for ambient measurements of Ammonia, Atmos. Meas. Tech., 3, 1075–1087, doi:10.5194/amt-3-1075-2010, 2010.

Berresheim, H., Elste, T., Plass-Dülmer, C., Eiseleb, F.L., and Tannerb, D.J.: Chemical ionization mass spectrometer for long-term measurements of atmospheric OH and H2SO4, International Journal of Mass Spectrometry, 202, 91–109, doi:10.1016/S1387-3806(00)00233-5, 2000.

Bianchi, F., Dommen, J., Mathot, S., and Baltensperger, U.: On-line determination of ammonia at low pptv mixing ratios in the CLOUD chamber, Atmos. Meas. Tech., 5, 1719–1725, doi:10.5194/amt-5-1719-2012, 2012.

Bianchi, F., Tröstl, J., Junninen, H., Frege, C., Henne, S., Hoyle, C. R., Molteni, U., Herrmann, E., Adamov, A., Bukowiecki, N., Chen, X., Duplissy, J., Gysel, M., Hutterli, M., Kangasluoma, J., Kontkanen, J., Kürten, A., Manninen, H. E., Münch, S., Peräkylä, O., Petäjä, T., Rondo, L., Williamson, C., Weingartner, E., Curtius, J., Worsnop, D. R., Kulmala, M., Dommen, J., and Baltensperger, U.: New particle formation in the free troposphere: A question of chemistry and timing, Science (New York, N.Y.), 352, 1109–1112, doi:10.1126/science.aad5456, 2016.

https://doi.org/10.5194/amt-2019-215
Preprint. Discussion started: 16 July 2019


Atmospheric Measurement Techniques Discussions

Bobrutzki, K. von, Braban, C. F., Famulari, D., Jones, S. K., Blackall, T., Smith, T. E. L., Blom, M., Coe, H., Gallagher, M., Ghalaieny, M., McGillen, M. R., Percival, C. J., Whitehead, J. D., Ellis, R., Murphy, J., Mohacsi, A., Pogany, A., Junninen, H., Rantanen, S., Sutton, M. A., and Nemitz, E.: Field inter-comparison of eleven atmospheric ammonia measurement techniques, Atmos. Meas. Tech., 3, 91–112, doi:10.5194/amt-3-91-2010, 2010.

Cubison, M. J. and Jimenez, J. L.: Statistical precision of the intensities retrieved from constrained fitting of overlapping peaks in high-resolution mass spectra, Atmos. Meas. Tech., 8, 2333–2345, doi:10.5194/amt-8-2333-2015, 2015.

Dunlop, P. J. and Bignell, C. M.: Prediction of the temperature dependence of binary diffusion coefficients of gaseous systems from thermal diffusion factors and diffusion coefficients at 300 K, International Journal of Thermophysics, 18, 939–945, doi:10.1007/BF02575239, 1997.

Dunne, E. M., Gordon, H., Kürten, A., Almeida, J., Duplissy, J., Williamson, C., Ortega, I. K., Pringle, K. J., Adamov, A., Baltensperger, U., Barmet, P., Benduhn, F., Bianchi, F., Breitenlechner, M., Clarke, A., Curtius, J., Dommen, J., Donahue, N. M., Ehrhart, S., Flagan, R. C., Franchin, A., Guida, R., Hakala, J., Hansel, A., Heinritzi, M., Jokinen, T., Kangasluoma, J., Kirkby, J., Kulmala, M., Kupc, A., Lawler, M. J., Lehtipalo, K., Makhmutov, V., Mann, G., Mathot, S., Merikanto, J., Miettinen, P., Nenes, A., Onnela, A., Rap, A., Reddington, C. L. S., Riccobono, F., Richards, N. A. D., Rissanen, M. P., Rondo, L., Sarnela, N., Schobesberger, S., Sengupta, K., Simon, M., Sipilä, M., Smith, J. N., Stozkhov, Y., Tomé, A., Tröstl, J., Wagner, P. E., Wimmer, D., Winkler, P. M., Worsnop, D. R., and Carslaw, K. S.: Global atmospheric particle formation from CERN CLOUD measurements, Science (New York, N.Y.), 354, 1119–1124, doi:10.1126/science.aaf2649, 2016.

Duplissy, J., Merikanto, J., Franchin, A., Tsagkogeorgas, G., Kangasluoma, J., Wimmer, D., Vuollekoski, H.,Schobesberger, S., Lehtipalo, K., Flagan, R. C., Brus, D., Donahue, N. M., Vehkamäki, H., Almeida, J., Amorim, A., Barmet, P., Bianchi, F., Breitenlechner, M., Dunne, E. M., Guida, R., Henschel, H., Junninen, H., Kirkby, J., Kürten, A., Kupc, A., Määttänen, A., Makhmutov, V., Mathot, S., Nieminen, T., Onnela, A., Praplan, A. P., Riccobono, F., Rondo, L., Steiner, G., Tome, A., Walther, H., Baltensperger, U., Carslaw, K. S., Dommen, J., Hansel, A., Petäjä, T., Sipilä, M., Stratmann, F., Vrtala, A., Wagner, P. E., Worsnop, D. R, Curtius, J., and Kulmala, M.: Effect of ions on sulfuric acid-water binary particle formation: 2. Experimental data and comparison with QC-normalized classical nucleation theory, *J. Geophys. Res. Atmos.*, 121, 1752– 1775, doi: 10.1002/2015JD023539, 2016.

Ehn, M., Thornton, J. A., Kleist, E., Sipilä, M., Junninen, H., Pullinen, I., Springer, M., Rubach, F., Tillmann, R., Lee, B., Lopez-Hilfiker, F., Andres, S., Acir, I.-H., Rissanen, M., Jokinen, T., Schobesberger, S., Kangasluoma, J., Kontkanen, J., Nieminen, T., Kurtén, T., Nielsen, L. B., Jørgensen, S., Kjaergaard, H. G., Canagaratna, M., Maso, M. D., Berndt, T., Petäjä, T., Wahner, A., Kerminen, V.-M., Kulmala, M., Worsnop, D. R., Wildt, J., and Mentel, T. F.: A large source of low-volatility secondary organic aerosol, Nature, 506, 476 EP -, doi:10.1038/nature13032, 2014.

Eisele, F. L. and Tanner, D. J.: Measurement of the gas phase concentration of H2SO4 and methane sulfonic acid and estimates of H2SO4 production and loss in the atmosphere, Journal of Geophysical Research: Atmospheres, 98, 9001–9010, doi:10.1029/93JD00031, 1993.

Eisele, F.L. and Hanson, D.R.: First Measurement of Prenucleation Molecular Clusters, The Journal of Physical Chemistry A, 104 (4), 830-836, doi:10.1021/jp9930651, 2000.

Elm, J., Passananti, M., Kurtén, T., and Vehkamäki, H.: Diamines Can Initiate New Particle Formation in the Atmosphere, The Journal of Physical Chemistry A, 121, 6155–6164, doi:10.1021/acs.jpca.7b05658, 2017.

Good, A., Durden, D. A., and Kebarle, P.: Mechanism and Rate Constants of Ion–Molecule Reactions Leading to Formation of H + (H 2 O) n in Moist Oxygen and Air, The Journal of Chemical Physics, 52, 222–229, doi:10.1063/1.1672668, 1970.

Hansel, A., Scholz, W., Mentler, B., Fischer, L., and Berndt, T.: Detection of RO 2 radicals and other products from cyclohexene ozonolysis with NH 4 + and acetate chemical ionization mass spectrometry, Atmospheric Environment, 186, doi:10.1016/j.atmosenv.2018.04.023, 2018.

Hanson, D. R., McMurry, P. H., Jiang, J., Tanner, D., and Huey, L. G.: Ambient pressure proton transfer mass spectrometry: detection of amines and ammonia, Environmental science & technology, 45, 8881–8888, doi:10.1021/es201819a, 2011.

Harald Stark, Reddy L.N. Yatavelli, Samantha L. Thompson, Joel R. Kimmel, Michael J. Cubison, Puneet S. Chhabra, Manjula R. Canagaratna, John T. Jayne, Douglas R. Worsnop, and Jose L. Jimenez: Methods to extract molecular and bulk chemical information from series of complex mass spectra with limited mass resolution, International Journal of Mass Spectrometry, 389, 26–38, doi:10.1016/j.ijms.2015.08.011, 2015.

Heinritzi, M., Simon, M., Steiner, G., Wagner, A. C., Kürten, A., Hansel, A., and Curtius, J.: Characterization of the mass-dependent transmission efficiency of a CIMS, Atmos. Meas. Tech., 9, 1449–1460, doi:10.5194/amt-9-1449-2016, 2016.

Höpfner, M., Volkamer, R., Grabowski, U., Grutter, M., Orphal, J., Stiller, G., Clarmann, T. von, and Wetzel, G.: First detection of ammonia (NH3) in the Asian summer monsoon upper troposphere, Atmos. Chem. Phys., 16, 14357–14369, doi:10.5194/acp-16-14357-2016, 2016.

Jen, C. N., Bachman, R., Zhao, J., McMurry, P. H., and Hanson, D. R.: Diamine-sulfuric acid reactions are a potent source of new particle formation, Geophys. Res. Lett., 43, 867–873, doi:10.1002/2015GL066958, 2016.

Jimenez, J. L., Canagaratna, M. R., Donahue, N. M., Prevot, A. S. H., Zhang, Q., Kroll, J. H., DeCarlo, P. F., Allan, J. D., Coe, H., Ng, N. L., Aiken, A. C., Docherty, K. S., Ulbrich, I. M., Grieshop, A. P., Robinson, A. L., Duplissy, J., Smith, J. D., Wilson, K. R., Lanz, V. A., Hueglin, C., Sun, Y. L., Tian, J., Laaksonen, A., Raatikainen, T., Rautiainen, J., Vaattovaara, P., Ehn, M., Kulmala, M., Tomlinson, J. M., Collins, D. R., Cubison, M. J., Dunlea, J., Huffman, J. A., Onasch, T. B., Alfarra, M. R., Williams, P. I., Bower, K., Kondo, Y., Schneider, J., Drewnick, F., Borrmann, S., Weimer, S., Demerjian, K., Salcedo, D., Cottrell, L., Griffin, R., Takami, A., Miyoshi, T., Hatakeyama, S., Shimono, A., Sun, J. Y., Zhang, Y. M., Dzepina, K., Kimmel, J. R., Sueper, D., Jayne, J. T., Herndon, S. C., Trimborn, A. M., Williams, L. R., Wood, E. C., Middlebrook, A. M., Kolb, C. E., Baltensperger, U., and Worsnop, D. R.: Evolution of Organic Aerosols in the Atmosphere, Science (New York, N.Y.), 326, 1525–1529, doi:10.1126/science.1180353, 2009.

https://doi.org/10.5194/amt-2019-215
Preprint. Discussion started: 16 July 2019

Jokinen, T., Sipilä, M., Junninen, H., Ehn, M., Lönn, G., Hakala, J., Petäjä, T., Mauldin III, R. L., Kulmala, M., and Worsnop, D. R.: Atmospheric sulphuric acid and neutral cluster measurements using CI-APi-TOF, Atmos. Chem. Phys., 12, 4117–4125, doi:10.5194/acp-12-4117-2012, 2012.

Jokinen, T., Sipilä, M., Kontkanen, J., Vakkari, V., Tisler, P., Duplissy, E.-M., Junninen, H., Kangasluoma, J., Manninen, H. E., Petäjä, T., Kulmala, M., Worsnop, D. R., Kirkby, J., Virkkula, A., and Kerminen, V.-M.: Ion-induced sulfuric acid\textendashammonia nucleation drives particle formation in coastal Antarctica, Science Advances, 4, doi:10.1126/sciadv.aat9744, 2018.

Kebarle, P.: Higher-Order Reactions--Ion Clusters and Ion Solvation, in: Ion-Molecule Reactions: Volume 1, Franklin, J. L. (Ed.), Springer US, Boston, MA, 315–362, 1972.

Kirkby, J., Curtius, J., Almeida, J., Dunne, E., Duplissy, J., Ehrhart, S., Franchin, A., Gagné, S., Ickes, L., Kürten, A., Kupc, A., Metzger, A., Riccobono, F., Rondo, L., Schobesberger, S., Tsagkogeorgas, G., Wimmer, D., Amorim, A., Bianchi, F., Breitenlechner, M., David, A., Dommen, J., Downard, A., Ehn, M., Flagan, R. C., Haider, S., Hansel, A., Hauser, D., Jud, W., Junninen, H., Kreissl, F., Kvashin, A., Laaksonen, A., Lehtipalo, K., Lima, J., Lovejoy, E. R., Makhmutov, V., Mathot, S., Mikkilä, J., Minginette, P., Mogo, S., Nieminen, T., Onnela, A., Pereira, P., Petäjä, T., Schnitzhofer, R., Seinfeld, J. H., Sipilä, M., Stozhkov, Y., Stratmann, F., Tomé, A., Vanhanen, J., Viisanen, Y., Vrtala, A., Wagner, P. E., Walther, H., Weingartner, E., Wex, H., Winkler, P. M., Carslaw, K. S., Worsnop, D. R., Baltensperger, U., and Kulmala, M.: Role of sulphuric acid, ammonia and galactic cosmic rays in atmospheric aerosol nucleation, Nature, 476, 429 EP -, doi:10.1038/nature10343, 2011.

Kirkby, J., Duplissy, J., Sengupta, K., Frege, C., Gordon, H., Williamson, C., Heinritzi, M., Simon, M., Yan, C., Almeida, J., Tröstl, J., Nieminen, T., Ortega, I. K., Wagner, R., Adamov, A., Amorim, A., Bernhammer, A.-K., Bianchi, F., Breitenlechner, M., Brilke, S., Chen, X., Craven, J., Dias, A., Ehrhart, S., Flagan, R. C., Franchin, A., Fuchs, C., Guida, R., Hakala, J., Hoyle, C. R., Jokinen, T., Junninen, H., Kangasluoma, J., Kim, J., Krapf, M., Kürten, A., Laaksonen, A., Lehtipalo, K., Makhmutov, V., Mathot, S., Molteni, U., Onnela, A., Peräkylä, O., Piel, F., Petäjä, T., Praplan, A. P., Pringle, K., Rap, A., Richards, N. A. D., Riipinen, I., Rissanen, M. P., Rondo, L., Sarnela, N., Schobesberger, S., Scott, C. E., Seinfeld, J. H., Sipilä, M., Steiner, G., Stozhkov, Y., Stratmann, F., Tomé, A., Virtanen, A., Vogel, A. L., Wagner, A. C., Wagner, P. E., Weingartner, E., Wimmer, D., Winkler, P. M., Ye, P., Zhang, X., Hansel, A., Dommen, J., Donahue, N. M., Worsnop, D. R., Baltensperger, U., Kulmala, M., Carslaw, K. S., and Curtius, J.: Ion-induced nucleation of pure biogenic particles, Nature, 533, 521 EP -, doi:10.1038/nature17953, 2016.

Kupc, A., Amorim, A., Curtius, J., Danielczok, A., Duplissy, J., Ehrhart, S., Walther, H., Ickes, L., Kirkby, J., Kürten, A., Lima, J. M., Mathot, S., Minginette, P., Onnela, A., Rondo, and Rondo, L.: A fibre-optic UV system for H2SO4 production in aerosol chambers causing minimal thermal effects, Journal of Aerosol Science, 42, 532–543, doi:10.1016/j.jaerosci.2011.05.001, 2011.

https://doi.org/10.5194/amt-2019-215
Preprint. Discussion started: 16 July 2019

Kurtén, T., Loukonen, V., Vehkamäki, H., and Kulmala, M.: Amines are likely to enhance neutral and ion-induced sulfuric acid-water nucleation in the atmosphere more effectively than ammonia, Atmos. Chem. Phys. Discuss., 8, 7455–7476, doi:10.5194/acpd-8-7455-2008, 2008.

Kürten, A.: New particle formation from sulfuric acid and ammonia: nucleation and growth model based on thermodynamics derived from CLOUD measurements for a wide range of conditions, Atmos. Chem. Phys.,19, 5033-5050, doi:10.5194/acp-19-5033-2019, 2019.

Kürten, A., Bergen, A., Heinritzi, M., Leiminger, M., Lorenz, V., Piel, F., Simon, M., Sitals, R., Wagner, A. C., and Curtius, J.: Observation of new particle formation and measurement of sulfuric acid, ammonia, amines and highly oxidized organic molecules at a rural site in central Germany, Atmos. Chem. Phys., 16, 12793–12813, doi:10.5194/acp-16-12793-2016, 2016b.

Kürten, A., Bianchi, F., Almeida, J., Kupiainen-Määttä, O., Dunne, E. M., Duplissy, J., Williamson, C., Barmet, P., Breitenlechner, M., Dommen, J., Donahue, N. M., Flagan, R. C., Franchin, A., Gordon, H., Hakala, J., Hansel, A., Heinritzi, M., Ickes, L., Jokinen, T., Kangasluoma, J., Kim, J., Kirkby, J., Kupc, A., Lehtipalo, K., Leiminger, M., Makhmutov, V., Onnela, A., Ortega, I. K., Petäjä, T., Praplan, A. P., Riccobono, F., Rissanen, M. P., Rondo, L., Schnitzhofer, R., Schobesberger, S., Smith, J. N., Steiner, G., Stozhkov, Y., Tomé, A., Tröstl, J., Tsagkogeorgas, G., Wagner, P. E., Wimmer, D., Ye, P., Baltensperger, U., Carslaw, K., Kulmala, M., and Curtius, J.: Experimental particle formation rates spanning tropospheric sulfuric acid and ammonia abundances, ion production rates, and temperatures, J. Geophys. Res. Atmos., 121, 12,377-12,400, doi:10.1002/2015JD023908, 2016a.

Kürten, A., Jokinen, T., Simon, M., Sipilä, M., Sarnela, N., Junninen, H., Adamov, A., Almeida, J., Amorim, A., Bianchi, F., Breitenlechner, M., Dommen, J., Donahue, N. M., Duplissy, J., Ehrhart, S., Flagan, R. C., Franchin, A., Hakala, J., Hansel, A., Heinritzi, M., Hutterli, M., Kangasluoma, J., Kirkby, J., Laaksonen, A., Lehtipalo, K., Leiminger, M., Makhmutov, V., Mathot, S., Onnela, A., Petäjä, T., Praplan, A. P., Riccobono, F., Rissanen, M. P., Rondo, L., Schobesberger, S., Seinfeld, J. H., Steiner, G., Tomé, A., Tröstl, J., Winkler, P. M., Williamson, C., Wimmer, D., Ye, P., Baltensperger, U., Carslaw, K. S., Kulmala, M., Worsnop, D. R., and Curtius, J.: Neutral molecular cluster formation of sulfuric acid-dimethylamine observed in real time under atmospheric conditions, Proceedings of the National Academy of Sciences of the United States of America, 111, 15019–15024, doi:10.1073/pnas.1404853111, 2014.

Kürten, A., Rondo, L., Ehrhart, S., and Curtius, J.: Performance of a corona ion source for measurement of sulfuric acid by chemical ionization mass spectrometry, Atmos. Meas. Tech., 4, 437–443, doi:10.5194/amt-4-437-2011, 2011.

Kürten, A., Rondo, L., Ehrhart, S., and Curtius, J.: Calibration of a Chemical Ionization Mass Spectrometer for the Measurement of Gaseous Sulfuric Acid, The Journal of Physical Chemistry A, 116, 6375–6386, doi:10.1021/jp212123n, 2012.

Lehtipalo, K., Yan, C., Dada, L., Bianchi, F., Xiao, M., Wagner, R., Stolzenburg, D., Ahonen, L. R., Amorim, A., Baccarini, A., Bauer, P. S., Baumgartner, B., Bergen, A., Bernhammer, A.-K., Breitenlechner, M., Brilke, S., Buchholz, A., Mazon, S. B., Chen, D., Chen, X., Dias, A., Dommen, J., Draper, D. C., Duplissy, J., Ehn, M., Finkenzeller, H., Fischer, L.,

Frege, C., Fuchs, C., Garmash, O., Gordon, H., Hakala, J., He, X., Heikkinen, L., Heinritzi, M., Helm, J. C., Hofbauer, V., Hoyle, C. R., Jokinen, T., Kangasluoma, J., Kerminen, V.-M., Kim, C., Kirkby, J., Kontkanen, J., Kürten, A., Lawler, M. J., Mai, H., Mathot, S., Mauldin, R. L., Molteni, U., Nichman, L., Nie, W., Nieminen, T., Ojdanic, A., Onnela, A., Passananti, M., Petäjä, T., Piel, F., Pospisilova, V., Quéléver, L. L. J., Rissanen, M. P., Rose, C., Sarnela, N., Schallhart, S., Schuchmann, S., Sengupta, K., Simon, M., Sipilä, M., Tauber, C., Tomé, A., Tröstl, J., Väisänen, O., Vogel, A. L., Volkamer, R., Wagner, A. C., Wang, M., Weitz, L., Wimmer, D., Ye, P., Ylisirniö, A., Zha, Q., Carslaw, K. S., Curtius, J., Donahue, N. M., Flagan, R. C., Hansel, A., Riipinen, I., Virtanen, A., Winkler, P. M., Baltensperger, U., Kulmala, M., and Worsnop, D. R.: Multicomponent new particle formation from sulfuric acid, ammonia, and biogenic vapors, Science Advances, 4, doi:10.1126/sciadv.aau5363, 2018.

Leifer, I., Melton, C., Tratt, D. M., Buckland, K. N., Clarisse, L., Coheur, P., Frash, J., Gupta, M., Johnson, P. D., Leen, J. B., van Damme, M., Whitburn, S., and Yurganov, L.: Remote sensing and in situ measurements of methane and ammonia emissions from a megacity dairy complex: Chino, CA, Environmental pollution (Barking, Essex 1987), 221, 37–51, doi:10.1016/j.envpol.2016.09.083, 2017.

Martin, N. A., Ferracci, V., Cassidy, N., and Hoffnagle, J. A.: The application of a cavity ring-down spectrometer to measurements of ambient ammonia using traceable primary standard gas mixtures, Appl. Phys. B, 122, 219, doi:10.1007/s00340-016-6486-9, 2016.

Murphy, D. M. and Koop, T.: Review of the vapour pressures of ice and supercooled water for atmospheric applications, Quarterly Journal of the Royal Meteorological Society, 131, 1539–1565, doi:10.1256/qj.04.94, 2005.

Norman, M., Hansel, A., and Wisthaler, A.: O2+ as reagent ion in the PTR-MS instrument: Detection of gas-phase ammonia, International Journal of Mass Spectrometry, 265, 382–387, doi:10.1016/j.ijms.2007.06.010, 2007.

Norman, M., Spierig, C., Wolff, V., Trebs, I., Flechard, C., Wisthaler, A., Schnitzhofer, R., Hansel, A., and Neftel, A.: Intercomparison of ammonia measurement techniques at an intensively managed grassland site (Oensingen, Switzerland), Atmospheric Chemistry and Physics Discussions, v.8, 19791-19818 (2008), 2009.

Nowak, J. B., Huey, L. G., Eisele, F. L., Tanner, D. J., Mauldin, R. L., Cantrell, C., Kosciuch, E., and Davis, D., Chemical ionization mass spectrometry technique for the detection of dimethylsulfoxide and ammonia, J. Geophys. Res., 107(D18), 4363, doi:10.1029/2001JD001058, 2002.

Nowak, J. B., Huey, L. G., Russel, A.G., Tian D., Neuman, J.A., Orsini, D., Sjostedt, S.J., Sullivan, A.P., Tanner, D.J., Weber, R.J., Nenes, A.,Edgerton, E., and Fehsenfeld, F.C., Analysis of urban gas phase ammonia measurements from the 2002 Atlanta Aerosol Nucleation and Real-Time Characterization Experiment (ANARChE), J. Geophys. Res., 111, D17308, doi:10.1029/2006JD007113, 2006.

Nowak, J., Neuman, J., Bahreini, R., A. Brock, C., M. Middlebrook, A., G. Wollny, A., Holloway, J., Peischl, J., B. Ryerson, T., and Fehsenfeld, F.: Airborne observations of ammonia and ammonium nitrate formation over Houston, Texas, J. Geophys. Res., 115, doi:10.1029/2010JD014195, 2010.

Nowak, J., Neuman, J., Kozai, K., G. Huey, L., Tanner, D., Holloway, J., B. Ryerson, T., Frost, G., McKeen, S., and Fehsenfeld, F.: A chemical ionization mass spectrometry technique for airborne measurements of ammonia, J. Geophys. Res., 112, D10S02, doi:10.1029/2006JD007589, 2007.

Pollack, I. B., Lindaas, J., Roscioli, J. R., Agnese, M., Permar, W., Hu, L., and Fischer, E. V.: Evaluation of ambient ammonia measurements from a research aircraft using a closed-path QC-TILDAS spectrometer operated with active continuous passivation, Atmos. Meas. Tech. Discuss., https://doi.org/10.5194/amt-2019-11, in review, 2019.

Pozzer, A., Tsimpidi, A. P., Karydis, V. A., Meij, A. de, and Lelieveld, J.: Impact of agricultural emission reductions on fine-particulate matter and public health, Atmos. Chem. Phys., 17, 12813–12826, doi:10.5194/acp-17-12813-2017, 2017.

Roscioli, J. R., Zahniser, M. S., Nelson, D. D., Herndon, S. C., and Kolb, C. E.: New Approaches to Measuring Sticky Molecules: Improvement of Instrumental Response Times Using Active Passivation, The journal of physical chemistry. A, 120, 1347–1357, doi:10.1021/acs.jpca.5b04395, 2016.

Simon, M., Heinritzi, M., Herzog, S., Leiminger, M., Bianchi, F., Praplan, A., Dommen, J., Curtius, J., and Kürten, A.: Detection of dimethylamine in the low pptv range using nitrate chemical ionization atmospheric pressure interface time-of-flight (CI-APi-TOF) mass spectrometry, Atmos. Meas. Tech., 9, 2135–2145, doi:10.5194/amt-9-2135-2016, 2016.

Sipilä, M., Sarnela, N., Jokinen, T., Henschel, H., Junninen, H., Kontkanen, J., Richters, S., Kangasluoma, J., Franchin, A., Peräkylä, O., Rissanen, M. P., Ehn, M., Vehkamäki, H., Kurten, T., Berndt, T., Petäjä, T., Worsnop, D., Ceburnis, D., Kerminen, V.-M., Kulmala, M., and O'Dowd, C.: Molecular-scale evidence of aerosol particle formation via sequential addition of HIO3, Nature, 537, 532 EP -, doi:10.1038/nature19314, 2016.

Sipilä, M., Sarnela, N., Jokinen, T., Junninen, H., Hakala, J., Rissanen, M. P., Praplan, A., Simon, M., Kürten, A., Bianchi, F., Dommen, J., Curtius, J., Petäjä, T., and Worsnop, D. R.: Bisulfate – cluster based atmospheric pressure chemical ionization mass spectrometer for high-sensitivity (< 100 ppqV) detection of atmospheric dimethyl amine: proof-of-concept and first ambient data from boreal forest, Atmos. Meas. Tech., 8, 4001–4011, doi:10.5194/amt-8-4001-2015, 2015.

Skrotzki, J.: High-accuracy multiphase humidity measurements using TDLAS: application to the investigation of ice growth in simulated cirrus clouds, Ruperto-Carola University of Heidelberg, Heidelberg, 2012.

Sunner, J., Nicol, G., and Kebarle, P.: Factors determining relative sensitivity of analytes in positive mode atmospheric pressure ionization mass spectrometry, Analytical Chemistry, 60, 1300–1307, doi:10.1021/ac00164a012, 1988.

Tang, M. J., Shiraiwa, M., Pöschl, U., Cox, R. A., and Kalberer, M.: Compilation and evaluation of gas phase diffusion coefficients of reactive trace gases in the atmosphere: Volume 2. Diffusivities of organic compounds, pressure-normalised mean free paths, and average Knudsen numbers for gas uptake calculations, Atmos. Chem. Phys., 15, 5585-5598, https://doi.org/10.5194/acp-15-5585-2015, 2015.

Timonen, H., Cubison, M., Aurela, M., Brus, D., Lihavainen, H., Hillamo, R., Canagaratna, M., Nekat, B., Weller, R., Worsnop, D., and Saarikoski, S.: Applications and limitations of constrained high-resolution peak fitting on low

resolving power mass spectra from the ToF-ACSM, Atmos. Meas. Tech., 9, 3263–3281, doi:10.5194/amt-9-3263-2016, 2016.

Vaittinen, O., Metsälä, M., Persijn, S., Vainio, M., and Halonen, L.: Adsorption of ammonia on treated stainless steel and polymer surfaces, Appl. Phys. B, 115, doi:10.1007/s00340-013-5590-3, 2014.

Verriele, M., Plaisance, H., Depelchin, L., Benchabane, S., Locoge, N., and Meunier, G.: Determination of 14 amines in air samples using midget impingers sampling followed by analysis with ion chromatography in tandem with mass spectrometry, Journal of environmental monitoring JEM, 14, 402–408, doi:10.1039/c2em10636a, 2012.

W.J. Massman: A review of the molecular diffusivities of H2O, CO2, CH4, CO, O3, SO2, NH3, N2O, NO, and NO2 in air, O2 and N2 near STP, Atmospheric Environment, 32, 1111–1127, doi:10.1016/S1352-2310(97)00391-9, 1998.

Wang, S., Nan, J., Shi, C., Fu, Q., Gao, S., Wang, D., Cui, H., Saiz-Lopez, A., and Zhou, B.: Atmospheric ammonia and its impacts on regional air quality over the megacity of Shanghai, China, Scientific reports, 5, 15842, doi:10.1038/srep15842, 2015.

Weissler, G. L.: Positive and Negative Point-to-Plane Corona in Pure and Impure Hydrogen, Nitrogen, and Argon, Phys. Rev., 63, 96–107, doi:10.1103/PhysRev.63.96, 1943.

Wilkinson, G. N. and Rogers, C. E.: Symbolic Description of Factorial Models for Analysis of Variance, Journal of the Royal Statistical Society. Series C (Applied Statistics), 22, 392–399, doi:10.2307/2346786, 1973.

Yan, C., Dada, L., Rose, C., Jokinen, T., Nie, W., Schobesberger, S., Junninen, H., Lehtipalo, K., Sarnela, N., Makkonen, U., Garmash, O., Wang, Y., Zha, Q., Paasonen, P., Bianchi, F., Sipilä, M., Ehn, M., Petäjä, T., Kerminen, V.-M., Worsnop, D. R., and Kulmala, M.: The role of H2SO4-NH3 anion clusters in ion-induced aerosol nucleation mechanisms in the boreal forest, Atmos. Chem. Phys., 18, 13231–13243, doi:10.5194/acp-18-13231-2018, 2018.

Yao, L., Wang, M.-Y., Wang, X.-K., Liu, Y.-J., Chen, H.-F., Zheng, J., Nie, W., Ding, A.-J., Geng, F.-H., Wang, D.-F., Chen, J.-M., Worsnop, D. R., and Wang, L.: Detection of atmospheric gaseous amines and amides by a high-resolution time-of-flight chemical ionization mass spectrometer with protonated ethanol reagent ions, Atmos. Chem. Phys., 16, 14527–14543, doi:10.5194/acp-16-14527-2016, 2016.

Yokelson, R. J.: Evaluation of adsorption effects on measurements of ammonia, acetic acid, and methanol, J. Geophys. Res., 108, 75, doi:10.1029/2003JD003549, 2003.

You, Y., Kanawade, V. P., Gouw, J. A. de, Guenther, A. B., Madronich, S., Sierra-Hernández, M. R., Lawler, M., Smith, J. N., Takahama, S., Ruggeri, G., Koss, A., Olson, K., Baumann, K., Weber, R. J., Nenes, A., Guo, H., Edgerton, E. S., Porcelli, L., Brune, W. H., Goldstein, A. H., and Lee, S.-H.: Atmospheric amines and ammonia measured with a chemical ionization mass spectrometer (CIMS), Atmos. Chem. Phys., 14, 12181–12194, doi:10.5194/acp-14-12181-2014, 2014.

Yu, F., Nadykto, A. B., Herb, J., Luo, G., Nazarenko, K. M., and Uvarova, L. A.: H2SO4–H2O–NH3 ternary ion-mediated nucleation (TIMN): kinetic-based model and comparison with CLOUD measurements, Atmos. Chem. Phys., 18, 17451–17474, doi:10.5194/acp-18-17451-2018, 2018.

https://doi.org/10.5194/amt-2019-215
Preprint. Discussion started: 16 July 2019

Atmospheric Measurement Techniques Discussions

Zhao, J. and Zhang, R.: Proton transfer reaction rate constants between hydronium ion (H3O+) and volatile organic compounds, Atmospheric Environment, 38, 2177–2185, doi:10.1016/j.atmosenv.2004.01.019, 2004.

800

https://doi.org/10.5194/amt-2019-215
Preprint. Discussion started: 16 July 2019

Atmospheric Measurement Techniques Discussions

Table 1. Estimated limits of detection (LOD) for some basic compounds and iodic acid measured with the water cluster CI-APi-TOF (in pptv). The LOD is derived by background measurements carried out at the CLOUD chamber, where LOD = 3•σ (You et al., 2014). σ is defined as the standard deviation of the background signal. The calculated detection limits are based on a 2.5 hour measurement at 278 K and 80% RH (averaging time of single data points: 1 minute). Additionally, the measured instrumental background mixing ratios (mean values) during this time period are provided (in pptv).

Detected compound	**LOD (pptv)**	**Instrumental background (pptv)**	**Measured *m/z* values (Th)**
NH_3 (ammonia)	0.5 ± 0.047	3.73 ± 0.353	18.0338 (NH_4^+); 36.0444 ($(H_2O)NH_4^+$)
C_2-amines (e.g., dimetylamine)	0.047 ± 0.004	0.058 ± 0.005	46.0651 ($(CH_3)_2NH_2^+$)
C_5H_5N (pyridine)	0.094 ± 0.009	< LOD	80.0495 ($(C_5H_5N)H^+$)
HIO_3 (iodic acid)	0.007	< LOD	176.9043 ($(HIO_3)H^+$); 194.9149 ($(HIO_3)H_3O^+$)

https://doi.org/10.5194/amt-2019-215
Preprint. Discussion started: 16 July 2019

Atmospheric Measurement Techniques Discussions

Table 2. Detected iodine containing signals in the water cluster CI-APi-TOF (sum formulas) spectra and the measured *m*/*z* values (in Th) during the CLOUD13 campaign.

Detected compound	Measured *m*/*z* value (Th)
I^+	126.9039
IO^+	142.8988
HIO^+	143.9067
IO_2^+	158.8938
$H_2IO_2^+$	160.9094
$H_3IO_2^+$	161.9172
$H_4IO_2^+$	162.9251
HIO_3^+	175.8965
$H_2IO_3^+$	176.9043
$H_3IO_3^+$	177.9121
$H_4IO_3^+$	178.9200
$H_4IO_4^+$	194.9149
$H_6IO_5^+$	212.9254
I_2^+	253.8084
$HI_2O_5^+$	334.7908
$H_3I_2O_5^+$	336.8064
$H_3I_2O_6^+$	352.8014
$H_5I_2O_6^+$	354.8170
$H_5I_2O_7^+$	370.8119
$H_2I_3O_7^+$	494.6929
$HI_3O_8^+$	509.6800
$H_2I_3O_8^+$	510.6878
$H_4I_3O_8^+$	512.7035
$H_4I_3O_9^+$	528.6984
$HI_4O_8^+$	636.5845
$HI_4O_9^+$	652.5794
$H_3I_4O_9^+$	654.5950
$H_3I_4O_{10}^+$	670.5900

https://doi.org/10.5194/amt-2019-215
Preprint. Discussion started: 16 July 2019

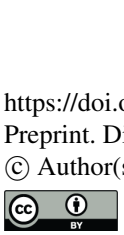

Atmospheric Measurement Techniques Discussions

$H_3I_4O_{11}^+$	686.5849

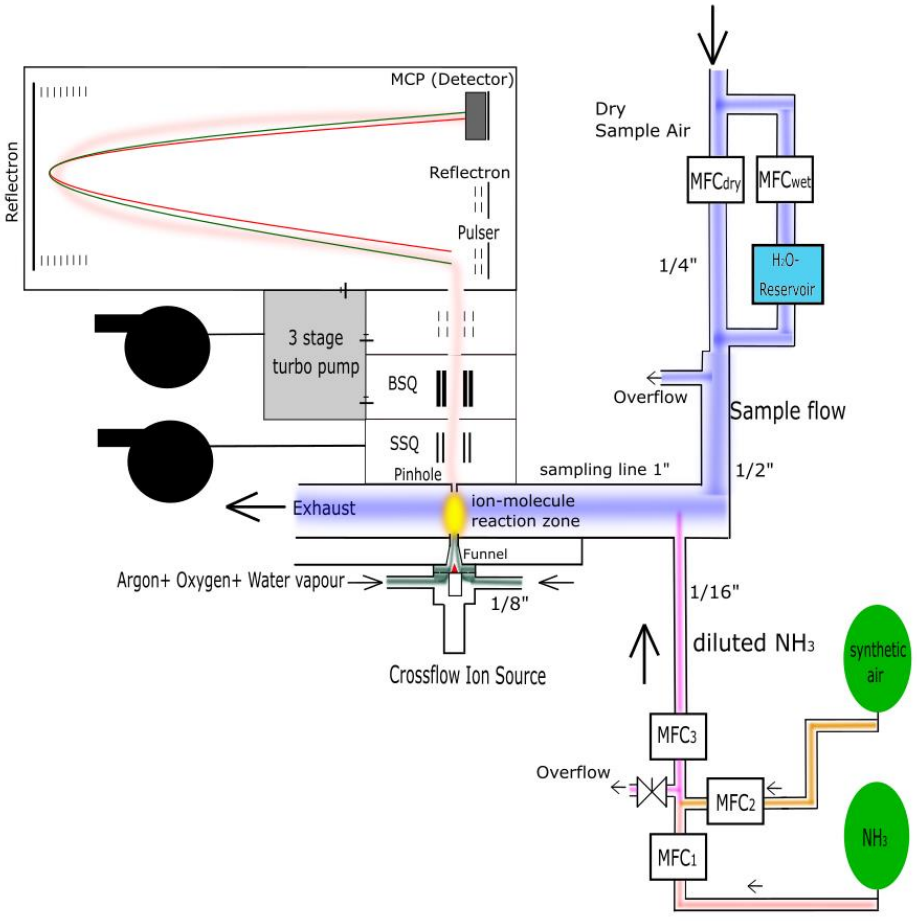

Figure 1: Experimental setup of the water cluster CI-APi-TOF during calibrations. The blue color indicates the sample flow. It consists of a mixture of 80% nitrogen and 20% oxygen. A portion of the sample flow can be humidified with a water bubbler (H_2O reservoir) to achieve different relative humidities. The calibration setup for ammonia consists of five mass flow controllers (MFCs) allowing two dilution steps at different humidity. Three MFCs (MFC_1, MFC_2, MFC_3) control the amount of ammonia that is added through a 1/16'' capillary into the center of the sample flow, where the second dilution stage occurs. The reagent ions (i.e., protonated water clusters) are produced when the ion source gas (argon, oxygen, water vapor) passes a corona needle at a positive high voltage (red triangle). The measured product ions are generated in the ion-molecule reaction zone (yellow area) at atmospheric pressure. After passing the pinhole, the ions are transported through two quadrupoles (Small Segmented Quadrupole, SSQ and Big Segmented Quadrupole, BSQ) towards the detection region of the mass spectrometer (Micro-Channel Plate, MCP; pressure is approx. 1×10^{-6} hPa). The calibration setup is disconnected during the measurements at the CLOUD chamber to reduce the instrumental background (leakage from the 1/16'' capillary).

https://doi.org/10.5194/amt-2019-215
Preprint. Discussion started: 16 July 2019

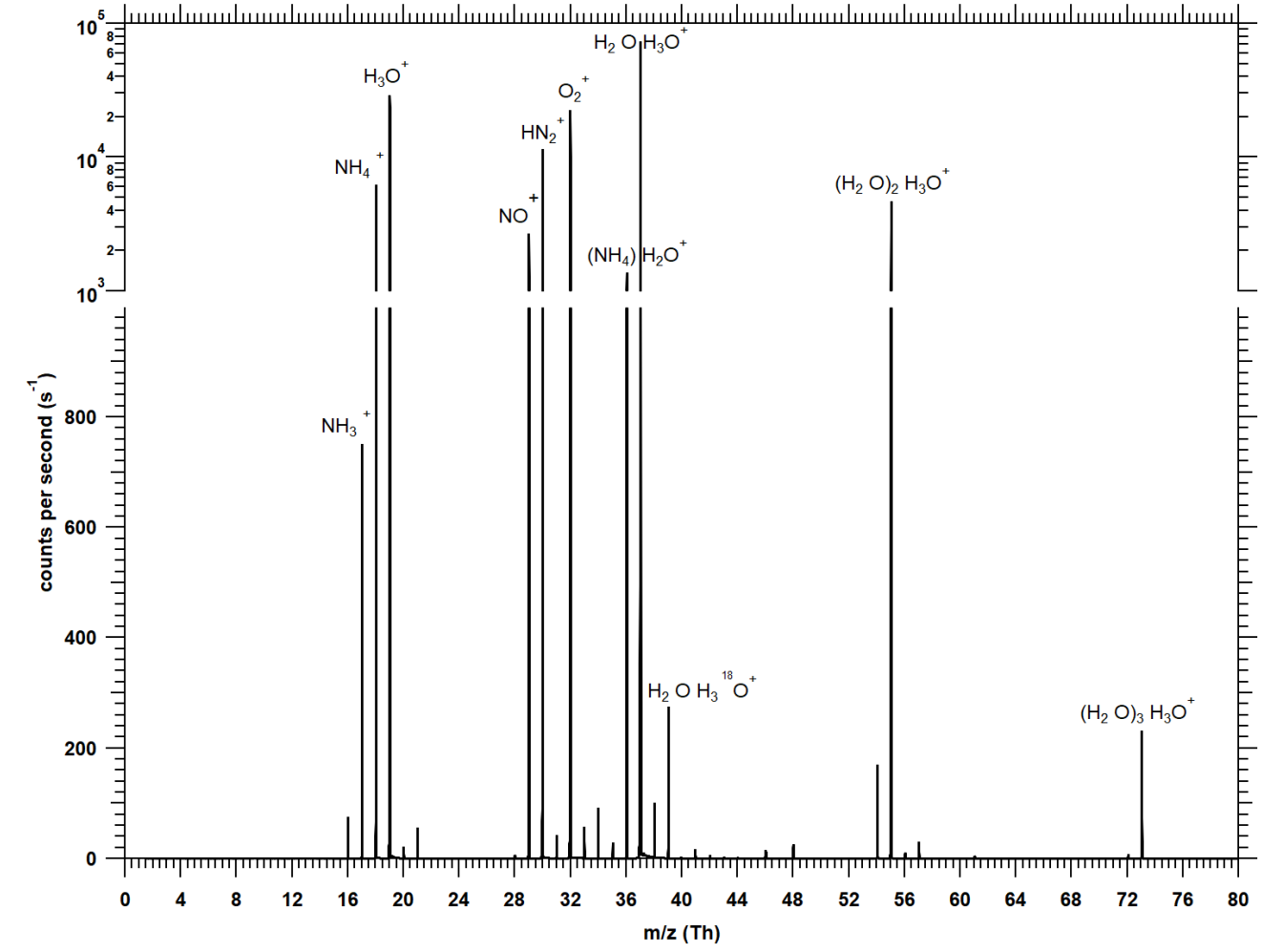

Figure 2: Typical mass spectrum recorded with the water cluster CI-APi-TOF when ca. 10 ppbv of ammonia are added during a calibration. Signals below 1000 counts per second are shown on a linear scale. The dominant signals (>1000 cps) are shown on a logarithmic scale. For the calculation of an ammonia mixing ratio the product ion signals (NH_4^+ and $(H_2O)NH_4^+$) are normalized against the most prominent reagent ion signals (H_3O^+, $(H_2O)H_3O^+$, $(H_2O)_2H_3O^+$, $(H_2O)_3H_3O^+$). Also larger water clusters are probably present in the ion-molecule reaction zone but a significant fraction of water seems to evaporate in the atmospheric pressure interface (behind the pinhole) of the instrument. Background peaks from N_2H^+, NO^+ and O_2^+ are always present but are neglected in the data evaluation. Due to the short reaction time (< 1 ms) in the ion-molecule reaction zone, the count rates of the reagent ions dominate the spectrum even at high ammonia mixing ratios.

https://doi.org/10.5194/amt-2019-215
Preprint. Discussion started: 16 July 2019

Atmospheric Measurement Techniques Discussions

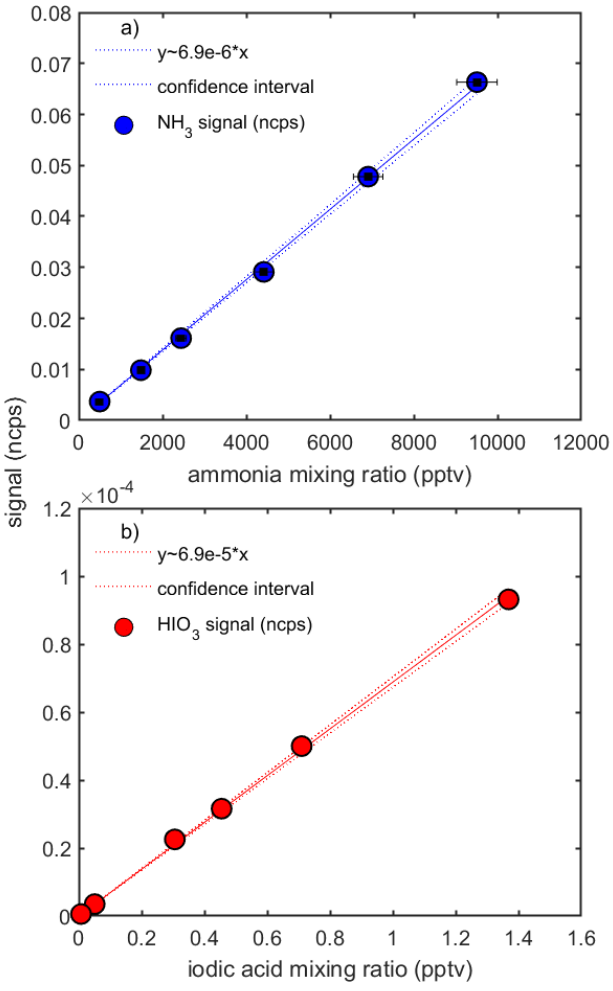

835 **Figure 3:** Calibration curves for ammonia (a) and iodic acid (b) at 40% relative humidity. The *y*-axes show the normalized counts per second (ncps) measured with the water cluster CI-APi-TOF; the mixing ratios of ammonia are determined from the calibration set-up and the iodic acid mixing ratios are taken from parallel measurements with a nitrate CI-APi-TOF at the CLOUD chamber. The inverse slopes from the linear fits yield the calibration factors (see equation (1) and (2)).

https://doi.org/10.5194/amt-2019-215
Preprint. Discussion started: 16 July 2019

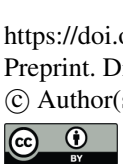

Atmospheric Measurement Techniques Discussions

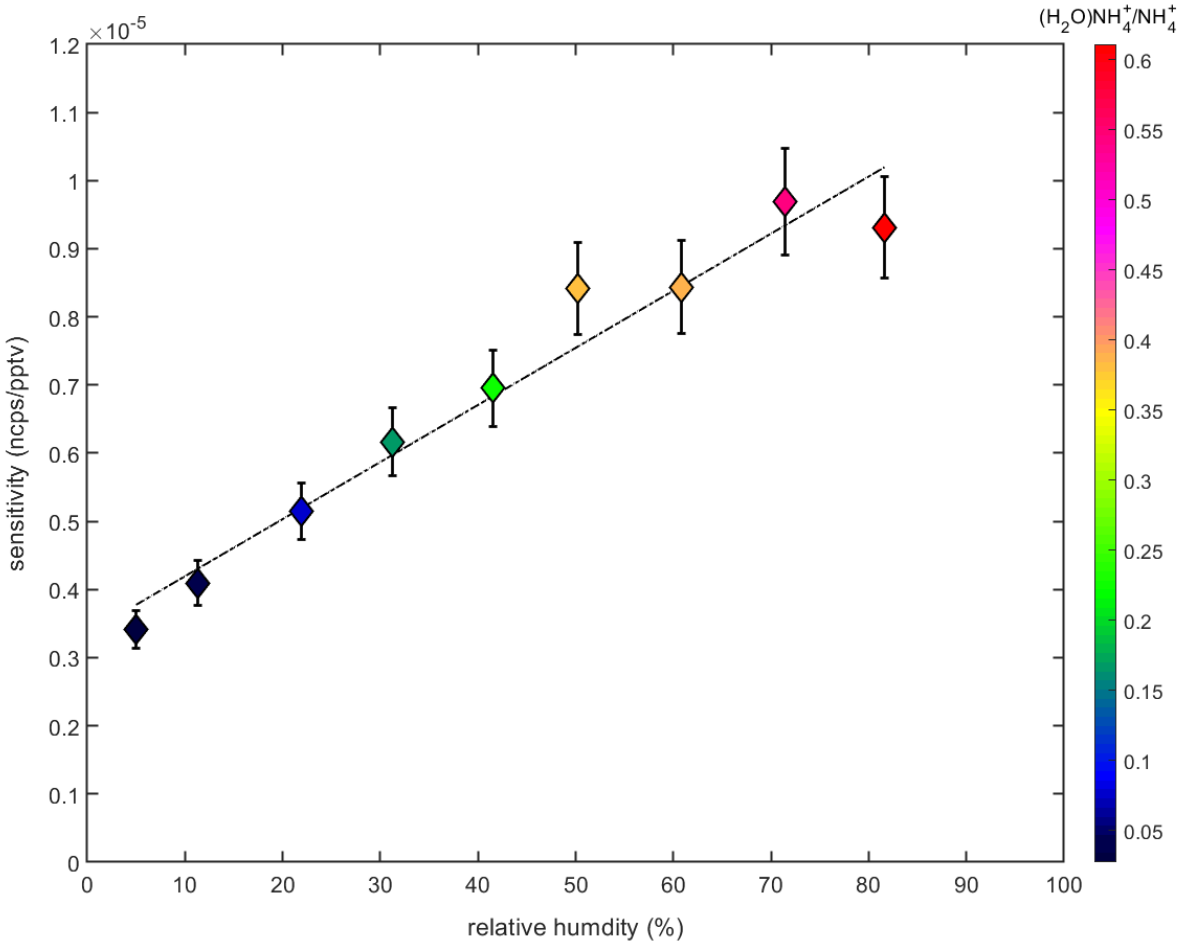

840

Figure 4: Dependency of the ammonia sensitivity as a function of the relative humidity (in %). A linear increase with relative humidity is observed that coincides with an increase of the ratio between the $(H_2O)NH_4^+$ and NH_4^+ ion signals (indicated by the color-code).

https://doi.org/10.5194/amt-2019-215
Preprint. Discussion started: 16 July 2019

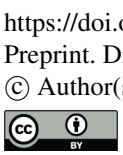

Atmospheric Measurement Techniques Discussions

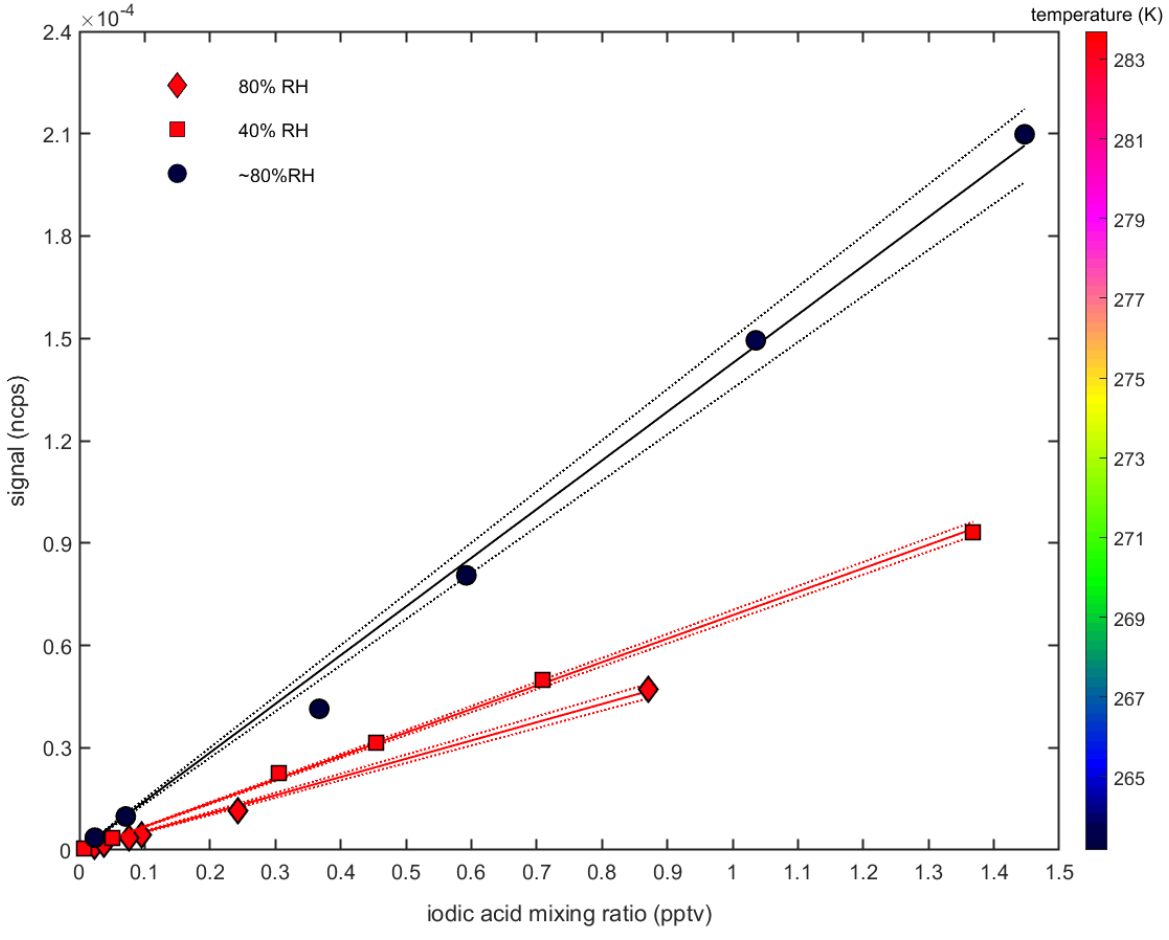

Figure 5: Calibration curves for iodic acid for different relative humidities and temperatures. The normalized counts per second (*y*-axis) are shown against the iodic acid mixing ratio measured with a nitrate CI-APi-TOF (*x*-axis) at the CLOUD chamber. The color code indicates the temperature inside the chamber. The sensitivity increases at lower temperatures, while no humidity dependency is observed for the relative humidities investigated during the experiments.

https://doi.org/10.5194/amt-2019-215
Preprint. Discussion started: 16 July 2019

Atmospheric Measurement Techniques Discussions

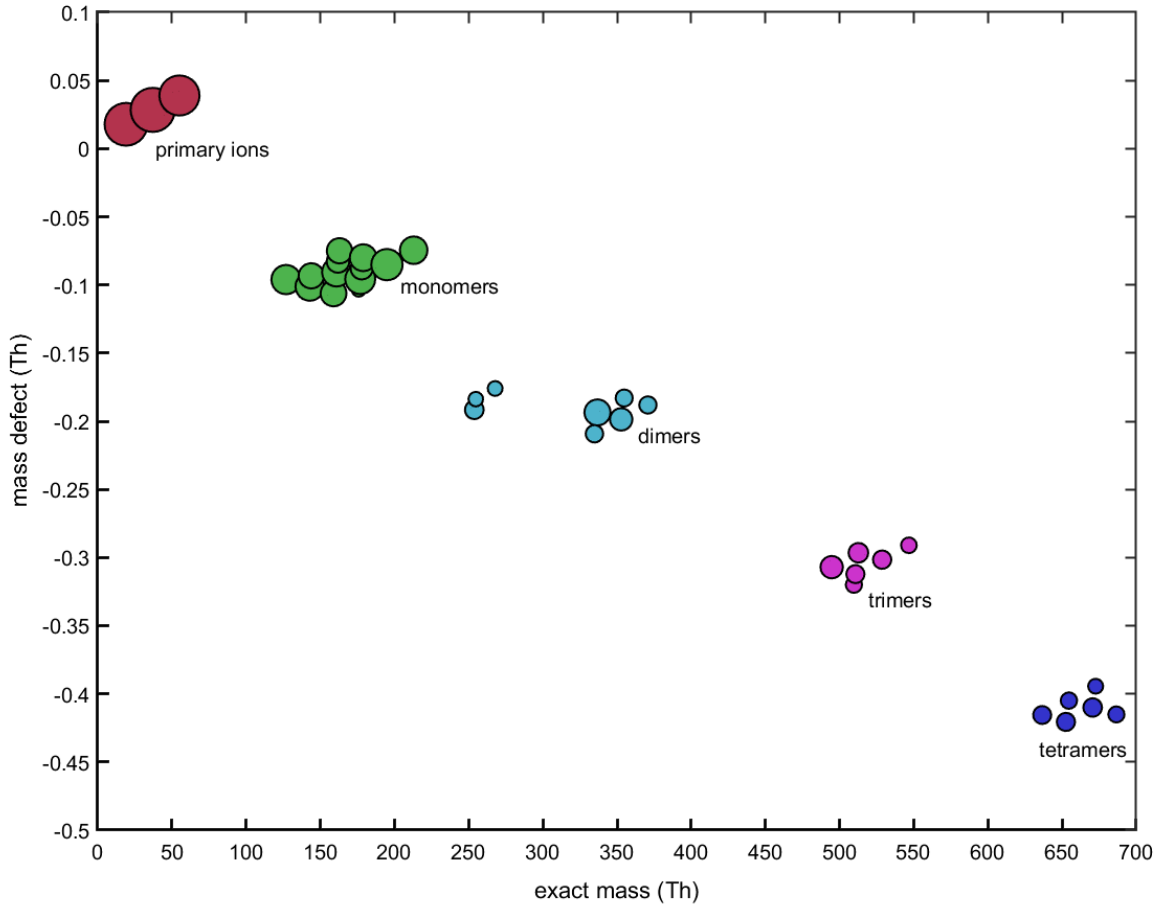

Figure 6: Detected iodine species and most prominent reagent ions during a CLOUD13 experiment shown as a mass defect plot. The iodine compounds result from I_2 photolysis and subsequent reactions during an experiment where new particle formation from iodine is studied. The estimated iodic acid mixing ratio is ~0.98 pptv. The *y*-axis shows the mass defects (in Th) of the identified compounds (see Table 2 and text for details), while the *x*-axis shows the absolute masses (in Th). The size of the symbols is proportional to the measured signal intensities (on a logarithmic scale). The notation monomers, dimers, trimers, and tetramers refers to the number of iodine atoms in the identified ions or clusters.

https://doi.org/10.5194/amt-2019-215
Preprint. Discussion started: 16 July 2019

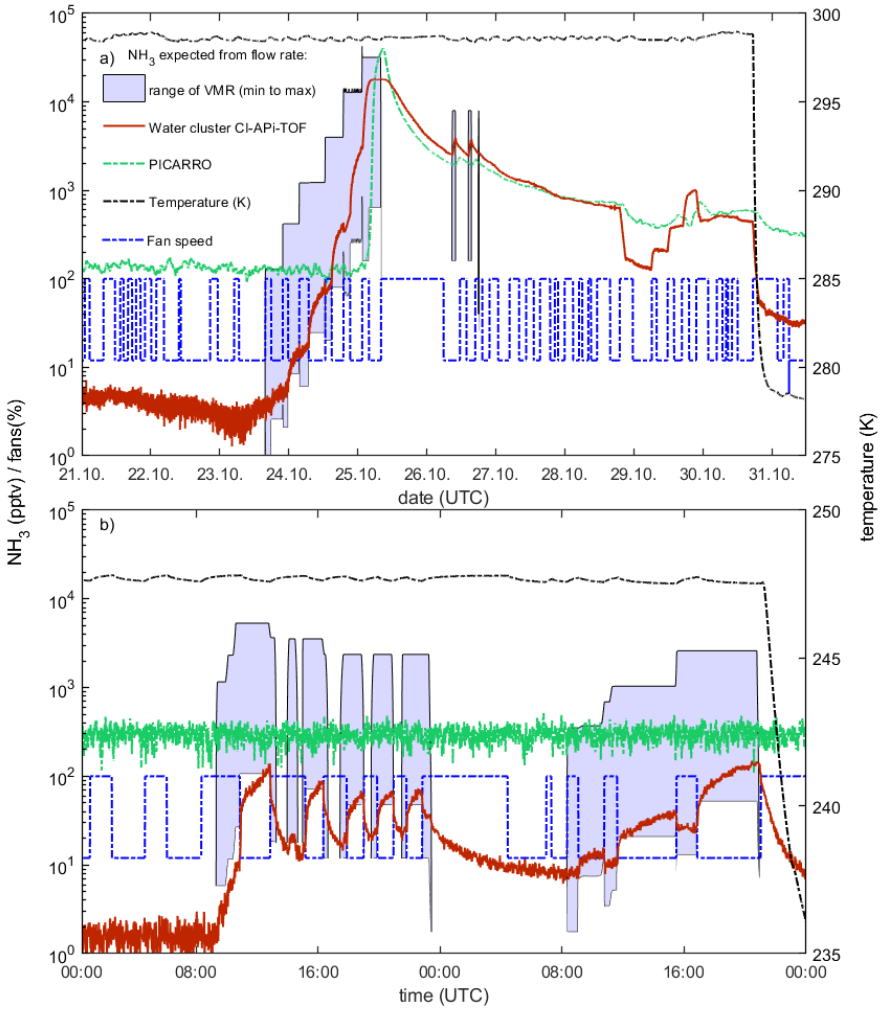

Figure 7: Inter-comparison between calculated (shaded blue area) and measured ammonia mixing ratios (PICARRO: solid green line; water cluster CI-APi-TOF: solid red line) inside the CLOUD chamber. The temperature inside the chamber is indicated by the dashed black line. The speed of two fans that mix the air inside the chamber is shown by the dashed blue line. The calculated ammonia mixing ratios (based on the flows of ammonia into the chamber) have a wide range due to uncertainties of the ammonia sink. We display the calculated range assuming that the chamber walls either act as a perfect sink (wall loss dominated, 25 s to 100 s lifetime depending on the fan speed) or no uptake of NH_3 occurs on the walls and the loss term is dilution dominated (~5000 s lifetime). During the experiments, the fan speed is varied between 12% and 100% (corresponding to ~48 and ~397 revolutions per minute). For higher fan speeds, the lifetime decreases due to increased turbulence inside the chamber. This effect is taken into account in the calculation of the minimum VMR, where a variability of the lifetime by a factor of 4 is assumed when the fan speed changes from 12% to 100%. The water cluster CI-APi-TOF reacts rapidly to changing conditions, such as variation of the ammonia flow into the chamber, temperature changes or different settings of the fan speed. See text for details.

https://doi.org/10.5194/amt-2019-215
Preprint. Discussion started: 16 July 2019

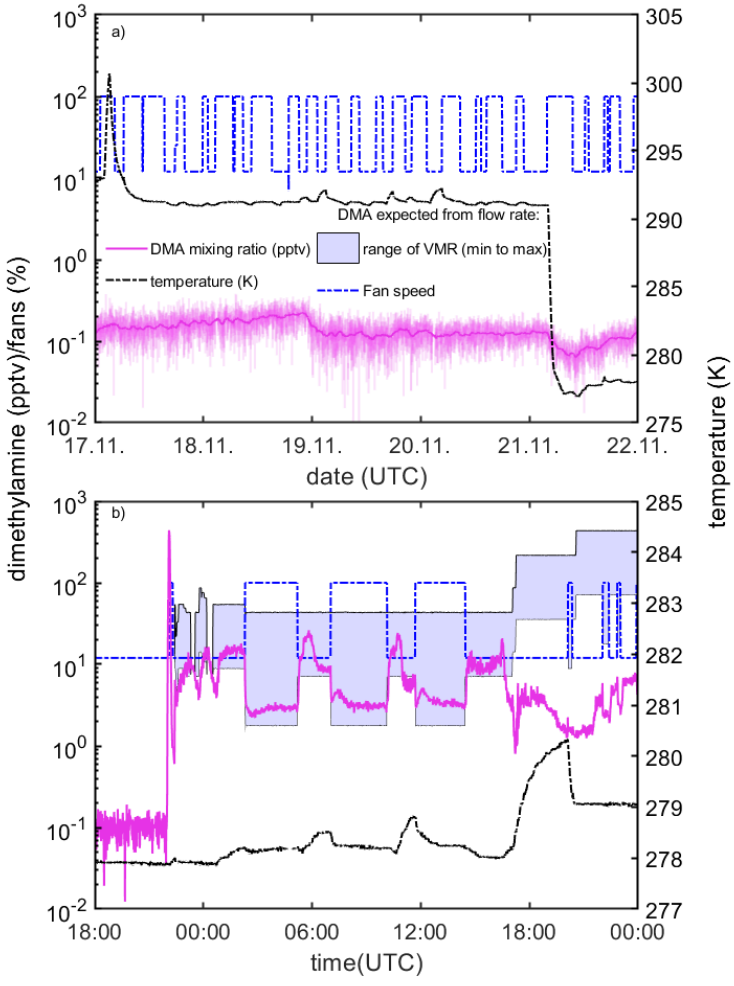

Figure 8: Measurement of the C_2-amine mixing ratio (in this case dimethylamine) during the CLOUD13 experiment. The pink line indicates the estimated mixing ratio of dimethylamine. The dashed black line shows the measured temperature inside the CLOUD chamber. The dashed blue lie shows the fan speed. Note that the mixing ratio of dimethylamine is calculated by using the calibration factor obtained for NH_3. A measurement of the chamber background over a time period of 5 days is shown in panel (a). The mean instrumental background during this time is at ~0.14 pptv (1 minute average data). The highlighted magenta line indicates a moving average of the background measurement. Panel (b) shows the measured signal of dimethylamine during several experimental runs, while dimethylamine is actively injected into the chamber. The shaded blue area shows the calculated mixing ratios of dimethylamine during these experiments. Fluctuations can be explained by changes in fan speed (dashed blue line) or by injection of high concentrations of other vapors (end of the time series; see text for details).